Scale in Remote Sensing and GIS

Edited by
Dale A. Quattrochi
National Aeronautics and Space Administration
Huntsville, Alabama
and
Michael F. Goodchild
University of California
Santa Barbara, California

LEWIS PUBLISHERS
Boca Raton New York London Tokyo

Cover: Color composite image of processed Landsat Thematic Mapper image recorded September 14, 1989 over the central Amazon River approximately 50 km upstream from the town of Óbidos and 650 km downstream from the town of Manaus. The record flood of 1989 has receded approximately 2 m, the floodplain is draining, and flow is from left to right (west to east) in the main channel which is 4 to 6 km wide. The color of the main channel (red) indicates relatively high suspended-sediment concentrations in the water. The dark blue color indicates relatively clear water, and blue-green indicates tropical forest. Image processing completed by A. K. Mertes, Department of Geography, University of California, Santa Barbara. Raw image provided by R. Almeida Filho of INPE, Brazil.

Acquiring Editor: Neil Levine
Project Editor: Joan Moscrop
Marketing Manager: Greg Daurelle
Direct Marketing Manager: Arline Massey
Cover design: Denise Craig
Manufacturing: Sheri Schwartz

Library of Congress Cataloging-in-Publication Data

Scale in remote sensing and GIS / edited by Dale A. Quattrochi and Michael F. Goodchild
p. cm.
Includes bibliographical references and index.
ISBN 1-56670-104-X
1. Geographic information systems. 2. Remote sensing. I. Quattrochi, Dale A.
II. Goodchild, Michael F.
G70.212.S28 1996
621.36'78—dc20 96-27156
CIP

International Standard Book Number 1-56670-104-X
Library of Congress Card Number 96-27156
Printed in the United States of America 1 2 3 4 5 6 7 8 9 0
Printed on acid-free paper

CHAPTER 9

Scaling Predicted Pine Forest Hydrology and Productivity Across the Southern United States

Steven G. McNulty, James M. Vose, and Wayne T. Swank

INTRODUCTION

Models are useful for integrating knowledge about forest ecosystem processes at different temporal and spatial scales. All models scales have some utility, from representing physiological processes at the fine scale, to providing a tool for predicting forest function across large geographic areas (Wessman, 1992). Just as each model scale has some utility, each scale also has unique limitations and problems in model parameterization, validation, and application. To properly use a model, assessing the model strengths and weaknesses is important.

The appropriate model depends on the question asked. Will the model be used locally or regionally? What types of data are available for parameterizing the model, and how accurate are these data? What is the effect of aggregating input data on model predictions? The answers to these questions determine which scale of modeling is the most appropriate and how model output should be interpreted.

The objective of this chapter is to examine how the aggregation of input data influences the predictive capabilities of forest process models across a changing spatial or temporal resolution. We will examine the influence of data aggregation on multiple-scale forest process model development, use, and validation, using PnET-IIS, a physiologically-based model for predicting forest hydrology and productivity at the stand, ecosystem, and regional scales. Overall model structure and data requirements are outlined and model use and limitations at three spatial scales are discussed.

MODEL SCALES

Assessment of forest ecosystem function encompasses processes that operate across a range of spatial and temporal scales. For example, the effects of temperature, soil water stress (SWS), or atmospheric carbon dioxide on net photosynthesis are often studied at the leaf level where measurements made over seconds are used to construct fine-scale physiology models. Some researchers had success in adapting fine-scale photosynthesis models to predict canopy photosynthesis for forest stands with daily climatic information (Running and Gower, 1991). The activity of developing stand level physiological models from fine-scale physiological models to make estimates at larger spatial and temporal scales is often called "bottom-up" scaling (Caldwell et al., 1993).

In contrast to stand-level physiological models, coarse-scale biogeochemical models are designed to estimate forest processes over large spatial scales at a coarse spatial and temporal resolution. These models represent generalized ecological processes and are usually extrapolated to a 100 to 1000 km^2 spatial resolution with monthly climate data. The models are often parameterized with data collected at coarse temporal scales, such as monthly leaf area, and validated with data collected at many widely separated sites (Melillo et al., 1993; McNulty et al., 1994). The approach of developing coarse-scale biogeochemical models with generalized representations of ecosystem processes is called "top-down" scaling (Caldwell et al., 1993). In regional assessments, coarse-scale biogeochemical models are easier to define compared to stand-level physiology models. However, coarse-scale models may not represent fine-scale physiological processes at larger spatial and temporal scales.

As spatial scale increased, the number of model input parameters decreased but the total database size generally increased. Conversely, as the spatial scale decreased, the number of model parameters generally increased. Large scale models are more useful for predicting functional trends across broad geographic areas, but may inaccurately predict ecosystem function at a particular site. Small scale models may predict ecosystem processes at the sites for which data exist, but insufficient data may often restrict the use of small scale models at the landscape or regional scale. Therefore, there is also a need for large scale models that require fewer input data, which can be applied across a region.

For this chapter, we have identified three spatial scales to test the influence of data aggregation on model predictions using PnET-II S. The stand, ecosystem and regional scale represent varying degrees of temporal and spatial data aggregation (Table 1). PnET-II S was originally designed as an ecosystem scale model. We will examine the influence of data aggregation on model predictions using three spatial scales for comparison.

Data Aggregation

Data aggregation must be considered when applying models above or below the scale for which the model was originally designed. Ideally, the model would be insensitive or operate linearly over the range of model input values (Band et al.,

Table 1 Relationships Between Modeling Scales

Scale	Data aggregation	Spatial area
Stand	low	1 to 10 ha
Ecosystem	moderate	10 to 1000 ha
Regional	high	>100,000 ha

1991). If the model is insensitive to an input parameter, then aggregating the value with increasing scale will have little influence on model predictions. Very insensitive parameters can be included in the model structure and need not be entered as an input variable. If the model operates linearly across the range of model input values, then aggregation of the model parameter values with increasing scale will have little bias on model predictions. However, if the model does not operate linearly, the change in data aggregation could increase or decrease model predictions. In this example, model inputs such as soil water holding capacity (SWHC) and the climate were aggregated as the spatial scale increased from the stand to region.

MODEL TESTING AND VALIDATION

Model validation is often an overlooked aspect of modeling, especially at large scales. At these scales, the data needed for model testing was distributed across a broad geographical area, which may not be reasonably collected by a single researcher. Large scale model testing is more likely to use preexisting data collected by groups of individuals, often over long periods. The data is often extrapolated to provide complete geographic coverage and temporally or spatially aggregated.

Comparison of independent model outputs is another method used to assess model accuracy, especially at large spatial scales where other forms of model testing are difficult. In this method, outputs of large scale models are compared with outputs of small scale models specifically designed for certain ecosystems. In this example of the influence of data aggregation on model predictions, we used both measured and independently predicted data to compare the influence of changing scale on model predictive capabilities, due to data aggregation.

MODEL STRUCTURE

PnET-IIS was used to examine the influence of data aggregation on predictions of productivity and hydrology. The model was spatially dimensionless but most of the equations in the model were derived from ecosystem-level studies. PnET-IIS (McNulty et al., 1994, 1996a, 1996b) was a derivation of the PnET-II model developed by Aber et al. (1995) which was used to predict forest hydrology and productivity in the northeastern U.S. PnET-IIS used site-specific soil water holding capacity, four monthly climate parameters (minimum and maximum air temperature, total precipitation, and solar radiation) and species-specific process coefficients. PnET-IIS predicted evapotranspiration (ET), water drainage and net primary productivity

(NPP) from the stand-level (<1 ha) to a 0.5° x 0.5° grid cell resolution (approximately 50 x 75 km) across the southern U.S. (McNulty et al., 1994, 1996a). The model calculated the maximum amount of leaf-area that could be supported on a site based on the soil, the climate, and parameters specified for the vegetative type. Leaf area was a major component in calculating NPP and water use. PnET-IIS assumed that all stands were fully stocked and that leaf area was equal to the maximum amount of foliage that could be supported due to soil and climate limitations. Predicted NPP was defined as total gross photosynthesis minus growth and maintenance respiration for leaf, wood, and root compartments. PnET-IIS calculated respiration as a function of the current and previous month's minimum and maximum air temperature. The optimal temperature for loblolly pine net photosynthesis varied from 23° to 27°C, and the maximum air temperature for gross photosynthesis ranged from 30° to 43°C (Strain et al., 1976). As air temperature increased beyond the optimal photosynthetic temperature, the respiration rate increased while gross photosynthesis increased slightly or decreased, so proportionally less net carbon per unit leaf area was fixed (Kramer, 1980). Total gross photosynthesis was a function of gross photosynthesis per unit leaf area, and leaf area. Changes in water availability and plant water demand placed limitations on leaf area produced, so as vapor pressure deficit and air temperature increased above optimal levels, leaf area and total gross photosynthesis decreased.

Annual transpiration was calculated from a maximum potential transpiration modified by plant water demand (a function of gross photosynthesis and plant water use efficiency). In the model, interception loss was a function of leaf area and total precipitation, and ET was equal to transpiration plus interception loss. Drainage was calculated as water in excess of ET and SWHC. If precipitation inputs exceeded plant water demand, the soil was first recharged to the SWHC and if water was still available, water was output as drainage. Monthly drainage was summed to estimate an annual water outflow.

Models designed for use at large spatial scales are based on many assumptions about forest structure and function (e.g., soil water storage and stand stocking). For any single forest stand, one or more of the assumptions may be inaccurate. The degree and type of assumption inaccuracy will affect the degree of error in the model predictions of hydrology and productivity. Specific assumptions are built into large scale models and they are not expected to predict annual hydrology and productivity for all sites and all years accurately. However, at the scale for which the model was developed (i.e., ecosystem scale), model predictions should generally correlate with site hydrology and productivity, because sampled sites cover a wide range of environmental conditions. If general relationships are not found between predicted and measured hydrology and productivity at the ecosystem level, the model logic is flawed.

Input Data for PnET-HS

PnET-IIS required three types of input data: soils, climate, and vegetation. Soil water holding capacity was the only site-specific soil data used as a model input. PnET-IIS required four monthly climatic drivers: average monthly minimum and

maximum air temperature, total monthly precipitation, and average monthly solar radiation. The model used generalized species-dependent vegetation coefficients that remained either constant across all sites (e.g., growing degree days to start and stop leaf and wood production, light extinction coefficients) (Table 2) or varied in relation to the climate and soils data (e.g., maximum air temperature for gross photosynthesis). No site-specific vegetation data, such as leaf area index or site stocking, were required to run PnET-IIS. The method of data acquisition, data structure, and data aggregation in the model depended on the spatial scale for the model. Specific input data aggregation and use are discussed under each of the three spatial modeling scales (i.e., stand, ecosystem, and region).

Table 2 PnET-IIS Model Parameters Used for Prediction of Productivity and Hydrology in Southern U.S. Pine Forests

	Parameter model	
Parameter name	Abbreviation	Default value
Light Extinction Coefficient	k	0.5
Foliar Retention time (years)		2.0
Leaf Specific Weight (g)		9.0
NetPsnMaxA (slope)		2.4
NetPsnMaxB (intercept)		0
Light half saturation (J m^2 sec^{-1})	HS	70
Vapor deficit efficiency constant	VPDK	0.03
Water-use-efficiency constant	WUE C	10.9
Canopy evaporation fraction		0.15
Soil water release constant	F	0.04
Maximum air temperature for photosynthesis (°C)	TMAX	variable
Optimal air temperature for photosynthesis (°C)	TOPT	variable
Change in historic air temperature (°C)	DTEMP	0
Change in historic precipitation (% difference)	DPPT	0

STAND-LEVEL MODELING

PnET-IIS used site-specific climate and soil water holding capacity, and species-specific vegetation coefficients. Therefore, genetic variations in species water use efficiency, respiration, or photosynthetic rates were not accounted for at the stand-level. Variations in stand stocking or stand age were also not included in the model. These limitations of the model did not necessarily constitute model deficiencies. The model was designed to be applied at a coarser scale where differences in stand stocking or genetic variation for the optimal air temperature for net photosynthesis could average out across a wide range of site conditions.

Ideally, the model would be defined, run, and validated against many well-studied stands. Unfortunately, very few stands exist that have detailed climate, growth, soils, and hydrology data to compare with PnET-IIS predictions. Therefore, we predicted

stand-level forest hydrology using climate and hydrologic data collected in a single well-studied pine forest.

Besides comparing model predictions with field measurements, we also compared PnET-IIS hydrologic predictions with hydrologic predictions from a detailed stand-level hydrologic model (PROSPER). Comparison of PnET-IIS hydrologic predictions with field measurements and PROSPER hydrologic predictions provided valuable information on PnET-IIS spatial limitations associated with climate data aggregation from daily to monthly values.

Stand Description

The stand, located at the Coweeta Hydrologic Laboratory in western North Carolina, was a 16.1 ha, 37-year-old plantation (WS1), with a southerly aspect, that spans an elevation range from 705 to 988 m. White pine (*Pinusstrobus*) was planted in 1957 at a spacing of 1.8 x 1.8 m. The stand has not been thinned or fertilized. In 1990, basal area was 53.2 m^2 ha^{-1} and density was 1,015 stems ha^{-1}. Soils were mesic Typic Hapludults of the Fannin soil series. Soil texture was fine sandy loam derived from mica schist and gneiss. A mean annual precipitation of 179 cm was evenly distributed throughout the year (Swift et al., 1988).

Hydrology

We used two comparisons to evaluate the primary hydrologic components (ET and drainage) of PnET-IIS at the stand-level. First, we compared annual measured streamflow and predicted drainage from PnET-IIS. Second, we compared ET estimates of PnET-IIS with a phenomenological model (PROSPER). The 1980s was a period of extreme climatic conditions (i.e., record dry and wet years) which provided a contrast of environmental driving variables and hydrologic response. At the stand-level, gauged watersheds provided a means of directly validating simulated streamflow, because ET was estimated by subtracting streamflow from precipitation (P-RO).

Hydrologic Modeling Using PROSPER

PROSPER, a phenomenological, one-dimensional model linked the atmosphere, vegetation, and soils. Plant and soil characteristics were combined in an ET surface characterized by a surface resistance to water vapor loss. The resistance was analogous to the relationship between stomatal resistance and leaf water potential, and depended on the water potential at the ET surface. Evapotranspiration was predicted by a combined energy balance-aerodynamic method (i.e., modified Penman-Monteith described in Swift et al., 1975).

PROSPER used electrical network equations to balance water allocation between vegetation and the three soil layers. The flows of water within and between the soil and the plant were a function of the soil hydraulic conductivity, soil water potential, root characteristics in each soil layer, and surface water potential. Water flux in unsaturated soil was governed by hydraulic conductivity, where hydraulic conductivity was estimated from the relationship between soil matric potential and moisture

content (Luxmoore, 1973). The model simulated daily ET and soil water redistribution between soil layers.

PROSPER required climatic inputs of solar radiation, precipitation, windspeed, air temperature, and vapor pressure. Except for solar radiation, data were collected from a climatic station bordering WS1. Solar radiation was measured at the main climate station in the valley bottom (300 m from the WS1) and extrapolated to WS1 using Swift's (1976) algorithm. The model required several vegetation (e.g., leaf area index, root distribution, resistance to vapor loss) and soil (e.g., soil moisture release curves, porosity, saturated hydraulic conductivity) parameters described in Goldstein et al. (1974) and Vose and Swank (1994). PROSPER (Goldstein et al., 1974) was used extensively at Coweeta, and many functional aspects of the model were derived from data and relationships established at Coweeta (Swift et al., 1975; Huff and Swank, 1985; Vose and Swank, 1994). The model did well at Coweeta in assessing ET and streamflow response to differences in vegetation type (Swift et al., 1975), clearcutting, and regrowth (Huff and Swank, 1985).

Hydrologic Measurements

The first order stream draining WS1 has a 90° V-notch weir that has been operating since 1934. Streamflow data was recorded every five minutes, and summed for each year. Annual streamflow was determined from the weir data for the period 1980 to 1989.

Comparisons of PnET-IIS vs. Measured Streamflow and Modeled ET

We compared predicted annual drainage with measured streamflow from 1980 to 1989 (Figure 1). PnET-IIS predicted drainage was poorly correlated with measured streamflow, especially for 1980, 1981, 1982, 1986, and 1989, and no obvious pattern for these discrepancies evolved. For example, 1986 was a record dry year, 1989 was a record wet year, and 1980 and 1982 were average precipitation years. When Aber and Federer (1992) compared PnET predicted drainage and measured streamflow across a range of stands they found good agreement; however, they did not assess the ability of PnET to model streamflow for multiple years within the same stand. By comparison, PROSPER predicted annual drainage was highly correlated with measured streamflow across the same period ($r^2 = 0.81$; $P < 0.0001$; Vose and Swank, 1994). Results of our analyses suggested that over relatively short temporal (i.e., annual) and small spatial scales (i.e., stand-level), PnET-IIS does not simulate the inter-annual streamflow dynamics. In addition, when averaged across the ten-year period, PnET-IIS estimates of drainage were 37% greater than measured streamflow, suggesting poor performance in predicting longer-term average streamflow as well. The increase in PnET-IIS 1989 predicted drainage was not observed in increased measured streamflow. PnET-IIS did not have a deep water storage component, so water not used by the plants was assumed to be lost as drainage. Much of the increased precipitation that occurred in 1989 may have gone toward recharging the depleted ground water table. During the 1985 to 1988 drought, PnET-IIS underpredicted ET compared to PROSPER. PnET-IIS did not have a deep water storage pool

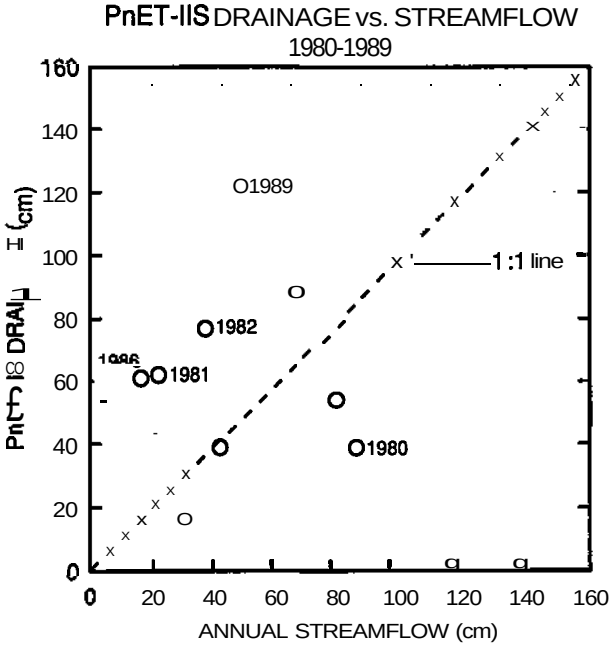

Figure 1 PnET-IIS predicted annual drainage vs. measured annual streamflow from Coweeta WS1 (1980 to 1989).

component to draw upon to supplement plant water demand as did PROSPER which predicted higher rates of ET during the drought.

Poor model performance may also be related to inaccurate stand-level estimates of ET. Because no procedure for directly measuring ET at the watershed scale exists, we compared PROSPER and PnET-IIS predicted ET to each other (Figure 2). The ET estimates from the two models did not agree, and the most dissimilar values occurred in 1980, 1985, 1987, and 1988. Three of these years (1985, 1987, and 1988) were extremely dry years (Swift et al., 1989) which may reflect a difference in the responsiveness of the models to dry conditions.

In addition to model structural limitations, the aggregation of daily climate data to monthly values for use in PnET-IIS could also have biased model predictions, especially during the drought years. Forests can rapidly respond to increased precipitation by increasing net photosynthesis and ET. The dynamics of forest response to isolated rain events during the drought caused PROSPER to predict more ET and less drainage compared with PnET-IIS predictions which used monthly climate.

Summary of Stand-Level Hydrology

PnET-IIS predictions of stand-level hydrology were poorly correlated with measured or PROSPER predicted hydrology. PnET-IIS failed to catch the change in ecosystem water use that can occur between climatic events (e.g., drought). The

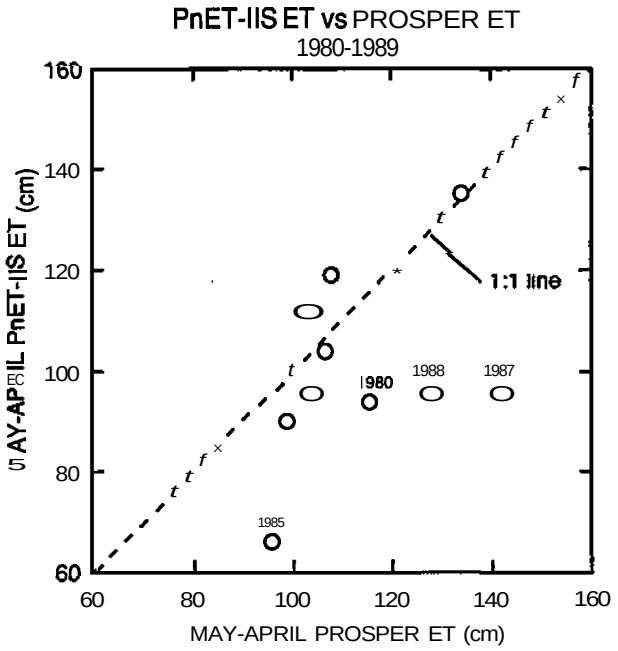

Figure 2 PnET-IIS predicted annual evapotranspiration (ET) vs. PROSPER predicted ET from Coweeta WS1 (1980 to 1989).

aggregation of daily climate data to monthly sums or averages may have reduced PnET-IIS sensitivity during extreme climatic events. Also, the lack of a deep soil water storage component reduced PnET-IIS predictions of ET during the drought.

This stand-level analysis showed the sacrifice made between available driving variables and model accuracy. Both the detail of the model and aggregation of input data influenced model predictions.

ECOSYSTEM-LEVEL FOREST MODELING

Modeling at the ecosystem level bridged the gap between stand-level models and regional-scale models. Ecosystem-level modeling had some commonality with stand-level modeling: (1) no spatial aggregation for climate model inputs; (2) model predictions were site-specific; and (3) productivity validation data was collected from specific sites. Ecosystem-level modeling also shared some common attributes with regional-scale models: (1) soil data was spatially aggregated; and (2) model predictions were located across a wide range of climate and soil conditions.

The structure of the model does not change between model scales (i.e., forest NPP and hydrology are still calculated using the same algorithms between scales). However, the source and amount of input data aggregation changed between scales.

Site Description

Ecosystem-level predictions of hydrology and productivity were run for 12 loblolly pine sites located across the southern U.S. (Figure 3). These sites represented a wide range of climate and soil conditions, and the sites met the following selection criteria: (1) sites were fully stocked at the time of sampling; (2) more than 95% of the stand basal area consisted of loblolly pine; (3) the site had not been thinned, burned, fertilized, or damaged by insect or disease; (4) all sites were on level terrain (<10% slope). PnET-IIS was run for each of the 12 sites using climate data from 1951 to 1990.

Ecosystem-Level Measurements of Forest Productivity

Measurement of total NPP can be both extremely laborious and destructive because the tree must be removed from the ground to measure root growth. Therefore, we used basal area growth as a surrogate for NPP. Two tree cores were collected 1.4 m above the forest floor (dbh), from each of 20 trees per site. The selected trees were randomly located within the plot, but represented the dominant or co-dominant size class. The first core was selected at a random azimuth, and the second core was extracted at 90° to the first core. Each core radius was measured from the outer growth ring to the pith. Annual tree ring widths were measured using a Model 3 Increment Measurer (Fred C. Henson Co., Mission Viejo, CA), which has an accuracy of 0.01 mm. Tree ring growth was converted to annual basal area growth (cm^2 $tree^{-1}$), and we assumed that the cross-sectional area of the bole is circular.

Input Data

Soil series data were derived from a geographic information system (GIS)-based soils atlas compiled by the Soil Conservation Service (Marx, 1988). The soil data was hand-digitized from a paper source at a scale between 1:500,000 and 1:1,500,000, depending on the state. Soil information associated with each series included SWHC to a depth of 102 cm. Because the locations of the soil types are not geographically precise, a 1-km area was overlaid on the soils coverage, centered around the latitude and longitude coordinate of each site. An aggregated weighted average of the SWHC within the area of each circle was used to assign a single SWHC for each site. All other soil parameter values were held constant across all sites and years (Table 1).

Three of the four climate parameters required by PnET-IIS were derived from the Forest Health Atlas, which provided cooperator and first-order station data from 1951 to 1984, and were originally acquired from the National Climatic Data Center (NCDC) (Marx, 1988). Cooperator station data include averaged minimum and maximum monthly air temperature, and total monthly precipitation, while first-order station records included relative humidity. Data from the three nearest climate stations next to each forest plot were averaged by month and the averaged value was assigned to the plot. The minimum and maximum air temperature, relative

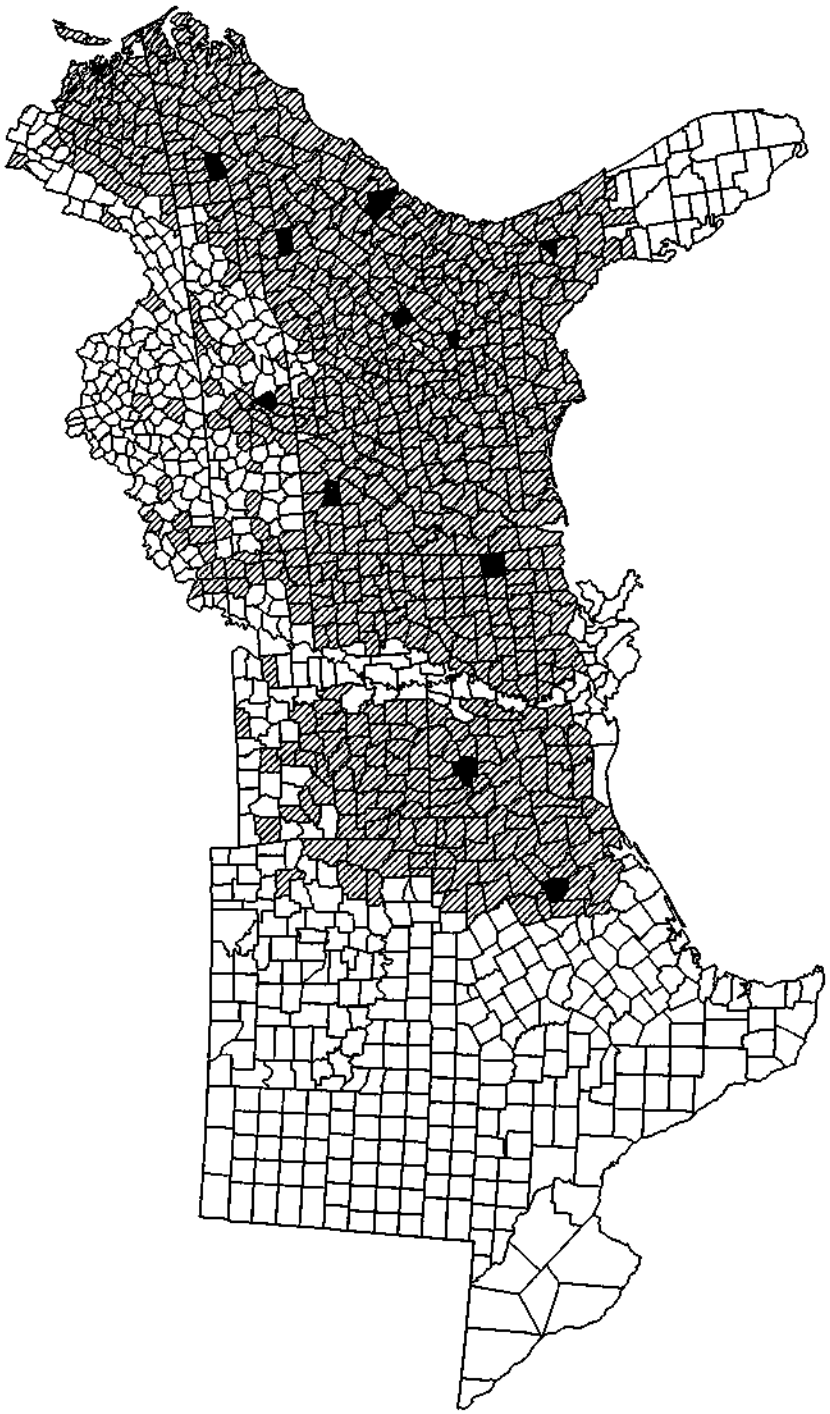

Figure 3 Site locations of the **12** pine sites sampled, overlaid on a range map of loblolly pine.

humidity, and precipitation databases were compiled into a single database and used to calculate average monthly solar radiation (Nikolov and Zeller, 1992) for each plot.

Climate data (i.e., air temperature, precipitation, and solar radiation) from 1985 to 1990 from the nearest three first-order or cooperator stations located closest to each of 12 sampled loblolly pine sites were extracted from NCDC microfiche. These data were averaged to estimate the climate for each site. The 1951 to 1984 and 1985 to 1990 climate databases were combined to produce an uninterrupted climate database from 1951 to 1990 (Table 3). The climate record for the ecosystem sites was longer than for the stand-level (i.e., 34 years vs. 10 years) and the drought experienced at Coweeta during the 1980s was much less severe across the region.

PnET-IIS Predicted Hydrology

Predicted annual ET ranged from 55.3 cm for 1988, at the Walker County, TX site, to 104.0 cm for 1979, at the Wayne County, MS site. The lowest average annual predicted ET occurred at the Glouchester County, VA site (mean = 69.1 cm H_2O, s.e. = 2.1, n = 14), and the highest average annual ET rate occurred at the Wayne County, MS site (mean = 94.1 cm H_2O, s.e. = 1.0, n = 28) (Table 4). Predicted annual drainage ranged from 5.2 cm for 1988 at the Walker County, TX site, to 86.0 cm for 1989 at the McMinn County, TN site. Average annual drainage was smallest in the Dooly County, GA site (mean = 29.5 cm, s.e. = 2.6, n = 11) and largest in the McMinn County, TN site (mean = 60.8 cm, s.e. = 5.6, n = 14) (Table 4).

Predictions of growing season soil water stress (GSSWS) ranged from 0.15 (no soil water stress) for various years on the Bradford County, FL, Glouchester County, VA, and the Wayne County, MS sites, to 0.63 for 1986 on the Dooly County, GA site and 0.68 for 1988 on the Walker County, TX site. The lowest predicted average annual GSSWS occurred on the Bradford County, FL site (mean = 0.17, s.e. = 0.02, n = 21), and the highest predicted average annual GSSWS occurred on the Dooly County, GA (mean = 0.44, s.e. = 0.04, n = 11) and Wilkinson County, GA sites (mean = 0.44, s.e. = 0.03, n = 13) (Table 4).

The lack of a severe region-wide drought, the wider range of site conditions, and the longer climate record may have improved the model's ability to predict forest hydrology accurately. However, because no site-level hydrologic measurements were recorded, we could not compare predicted and measured hydrology.

PnET-IIS Predicted vs. Measured Forest Growth

Predicted NPP ranged from 2.4 t ha^{-1} yr^{-1} for 1978 at the Walker County, TX site to 18.6 t ha^{-1} yr^{-1} for 1975 at the Wayne County, MS site. Average NPP across all sites equaled 11.3 t ha^{-1} yr^{-1}. Predicted average annual NPP was largest on the Colleton County, SC and Wayne County, MS sites, and NPP were smallest in the Dooly County, GA, McMinn County, TN, and the Wilkinson County, GA sites (Table 4).

The years of record (YOR) that basal area growth could be compared with predicted NPP varied between sites, because the date of plantation establishment and rate of canopy closure differed between sites (Table 3). The shortest record of

Table 3 Climatic Data for 12 Loblolly Pine Sites

Site	YOR	Lat. (°)	Grow. seas. avg. solar radiation (j m^{-1} sec^{-1})	Grow. seas. avg. temp. (°C)	Annual avg. temp. (°C)	Grow. seas. avg. PPT (cm H_2O)	Annual avg. PPT (cm H_2O)	GIS SWHC (cm H_2O 102 cm^{-1} soil)	Avg. basal area growth (cm^2 yr^{-1})
Bradford, FL	21	30.0	465 (10)	25.3 (0.2)	20.2 (0.2)	80 (2)	130 (3)	6	11.4 (0.5)
Bienville, LA	15	32.3	446 (5)	24.3 (0.2)	18.0 (0.2)	67 (7)	149 (9)	14	11.3 (0.9)
Chatham, NC	14	35.6	414 (6)	21.8 (0.1)	15.0 (0.2)	61 (4)	117 (6)	14	11.8 (0.5)
Chester, SC	8	34.8	432 (10)	22.6 (0.2)	16.2 (0.3)	66 (5)	120 (6)	13	13.1 (0.4)
Colleton, SC	11	32.9	436 (6)	24.5 (0.2)	18.7 (0.2)	68 (3)	121 (4)	13	21.1 (1.3)
Gloucester, VA	13	37.5	400 (7)	22.0 (0.2)	15.0 (0.3)	62 (4)	117 (7)	12	11.7 (0.7)
Dooly, GA	11	32.1	466 (8)	26.6 (0.2)	20.2 (0.3)	50 (2)	108 (4)	14	8.7 (0.8)
McMinn, TN	14	35.5	417 (9)	21.7 (0.2)	14.8 (0.2)	63 (6)	134 (9)	9	11.3 (0.7)
Morgan, AL	10	34.5	424 (9)	21.8 (0.2)	15.0 (0.2)	63 (4)	136 (5)	14	13.6 (0.4)
Walker, TX	12	31.0	477 (8)	25.3 (0.3)	19.5 (0.2)	55 (2)	114 (7)	11	14.2 (1.6)
Wayne, MS	28	31.6	432 (4)	24.1 (0.2)	18.2 (0.2)	72 (3)	149 (6)	16	17.4 (0.7)
Wilkinson, GA	14	32.8	449 (6)	24.0 (0.6)	17.9 (0.2)	50 (3)	111 (4)	13	11.4 (0.6)

Note: YOR = years of record between canopy closure and plot sampling, Lat. = latitude, Growing Seas. Avg. Solar Radiation = growing season solar radiation, SWHC= site soil water holding capacity derived from a Soil Conservation Service map of the soils on each site, Avg. Basal area growth = average annual basal area growth for the trees on each site. Standard errors are included in ( ).

Table 4 Predictions of Growing Season Evapotranspiration (ET), Drainage and Soil Water Stress (GSSWS) and Annual Evapotranspiration, Drainage and NPP for the 12 Measured Loblolly Pine Sites

	Average growing season			Average annual		
Site (state, county)	ET (cm)	Drainage (cm)	GSSWS (%)	ET (cm)	Drainage (cm)	NPP t biomass ha^{-1}
Bradford, FL	51.8 (1.5)	28.0 (1.9)	0.17 (0.02)	83.0 (1.7)	47.6 (2.6)	11.4 (0.9)
Bienville, LA	55.4 (1.1)	12.7 (2.7)	0.37 (0.03)	83.0 (1.4)	53.6 (4.6)	10.2 (0.7)
Chatham, NC	54.1 (1.1)	11.2 (1.4)	0.35 (0.05)	73.6 (1.4)	43.2 (3.2)	10.8 (0.9)
Chester, SC	51.7 (2.0)	12.1 (1.8)	0.37 (0.08)	73.8 (2.1)	46.0 (4.2)	10.3 (1.3)
Colleton, SC	56.4 (1.6)	14.5 (1.3)	0.31 (0.05)	83.1 (1.3)	38.5 (2.6)	12.8 (1.2)
Gloucester, VA	51.7 (1.3)	15.6 (1.8)	0.30 (0.05)	69.1 (1.4)	48.2 (3.9)	10.8 (0.9)
Dooly, GA	50.8 (1.9)	6.7 (0.5)	0.44 (0.03)	79.1 (1.4)	29.5 (2.6)	9.4 (0.8)
McMinn, TN	50.3 (1.5)	15.1 (3.2)	0.26 (0.04)	70.3 (1.3)	60.8 (5.6)	9.3 (0.8)
Morgan, AL	56.7 (1.4)	14.3 (2.0)	0.33 (0.05)	79.8 (1.5)	59.0 (4.4)	11.9 (0.9)
Walker, TX	48.1 (1.7)	11.3 (1.8)	0.38 (0.05)	76.0 (2.1)	39.8 (3.7)	9.9 (0.8)
Wayne, MS	62.6 (0.7)	15.2 (1.6)	0.28 (0.03)	94.1 (0.8)	55.2 (2.9)	13.1 (0.5)
Wilkinson, GA	51.9 (1.6)	6.2 (0.5)	0.44 (0.05)	76.9 (1.6)	34.3 (2.2)	9.1 (0.8)
Average	54.2 (0.5)	14.5 (0.6)	0.32 (0.01)	80.3 (0.7)	47.2 (1.2)	11.0 (0.3)

Note: Standard errors are included in ( ).

basal area growth was from the Chester County, SC site and the longest was from the Wayne County, MS site. Basal area growth ranged between 4.5 $cm^2\ tree^{-1}$ for 1980 at the Bienville Parish, LA site, to 26.4 $cm^2\ tree^{-1}$ for 1982 at the Colleton County, SC site. The Colleton County, SC site also had the largest average annual basal area growth, while the Dooly County, GA site had the smallest average annual basal area growth (Table 3).

Across all sites and years, predicted NPP was significantly correlated with annual basal area growth (Figure 4) ($r^2 = 0.30$, $P < 0.005$, $n = 165$). Average annual basal area growth was highly correlated ($r^2 = 0.66$, $P < 0.005$, $n = 12$) with average annual predicted NPP (Figure 5). Predicted NPP may be more closely related to average annual basal area across all sites when compared with inter-annual basal area growth because factors that influenced growth averaged out over time. For example episodic O_3 events influence the growth of loblolly pine (Kress et al., 1992; Faulkner et al., 1990), but O_3 was not accounted for by PnET-IIS. Additionally, changes in C allocation associated with NPP are not accounted for by basal area measurements alone.

Data Aggregation

Previous sensitivity analysis showed that PnET-IIS was insensitive to changes in SWHC (McNulty et al., 1996c). Therefore, aggregating SWHC for each site should have added little bias to model predictions' hydrologic predictions. At the ecosystem scale, we were not able to validate PnET-IIS predictions of drainage or ET, so we could not test this hypothesis on these sites.

Predicted NPP was significantly correlated with basal area growth but we could not plot a 1:1 relationship since these variables represent different measurements.

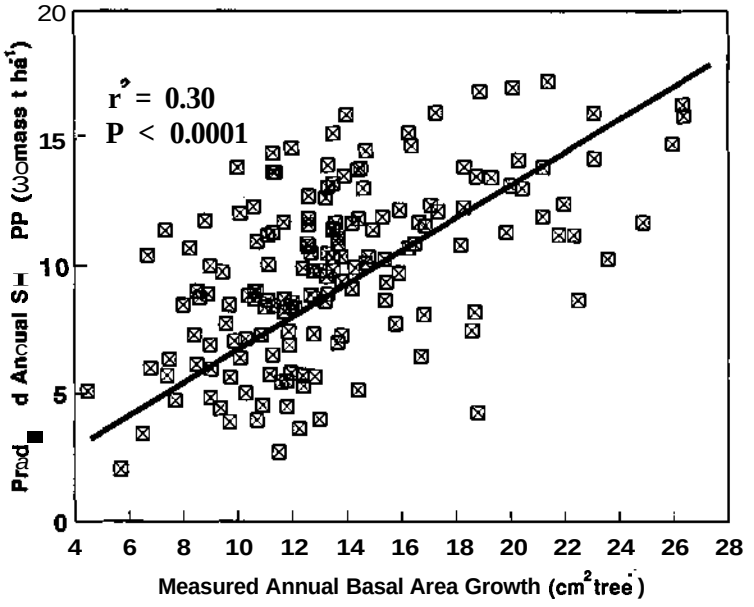

Figure 4 Annual predicted NPP vs. annual measured basal area growth for all 12 measured loblolly pine sites and years.

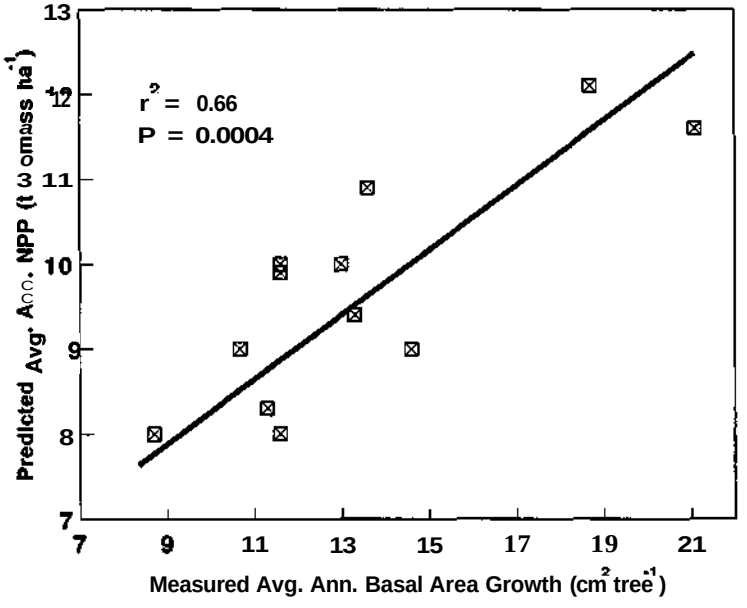

Figure 5 Average annual predicted NPP vs. average annual measured basal area growth for all 12 loblolly pine sites.

The aggregation of the daily to monthly climate data may have biased the estimates of NPP, but compared with basal area growth the bias seemed linear (Figure 4).

Summary of Ecosystem Modeling

Individually, predicted NPP was better correlated with basal area growth on some sites compared to other sites (McNulty et al., 1996b). However, across all sites, predicted NPP was significantly correlated with measured basal area growth (Figure 4). The drought described under the stand-level modeling section was not as long or as severe across the rest of the southern U.S. The lack of a deep soil water holding pool and aggregation of the daily to monthly climate may have been less detrimental to model predictions of NPP at the ecosystem scale because model prediction errors were offset across the wide range of site conditions.

REGIONAL-SCALE FOREST MODELING

Regional-scale models can offer valuable insight on forest function over large spatial areas, but there is often a lack of regional-scale contiguous input data. The data are often derived from many sources with varying degrees of associated error and completeness. Before the data can be used for modeling, the data must be screened for errors and extrapolated across the geographic range. Data aggregation, as previously discussed, is also a problem at the regional scale.

Input Data

Regional-scale PnET-IIS modeling required the same three types of input data (climate, soils, and vegetation) needed for stand- and ecosystem-level predictions. Only the source of the data and data aggregation changed between model scales.

Climate Data

To predict monthly loblolly pine growth and hydrology at a regional level, climate data from 1951 to 1984 were used as model inputs. The 900+ cooperative climate stations point databases were interpolated on a 0.5° x 0.5° grid across the southern U.S. (Marx, 1988). Each cell within the grid represented a spatial extent of 50 x 75 km. The gridded databases of average minimum and maximum monthly air temperature, average monthly relative humidity, and total precipitation were compiled into a single database and used to calculate average monthly solar radiation (Nikolov and Zeller, 1992).

Besides temporal aggregation of climate data (i.e., daily to monthly values), the regional model also aggregated the climate data spatially. The problem of parameter averaging increases with spatial scale (Band et al., 1991) and spatial aggregations of both air temperature precipitation are most pronounced along areas of topographic change. For example, in the southern U.S., the cool, moist climate of the Appalachian Mountains contrasts sharply with the hot, drier climate of the southern Coastal Plain.

The Appalachian Mountains are too cool to support southern pine, while air temperature may be above optimal for maximum pine productivity in the southern Coastal Plain. However, at large spatial scales, the cool mountain climate and the very warm coastal plain climate were averaged to create a false ideal climate suitable for pine growth.

Vegetation Inputs

Like for the stand- and ecosystem-level modeling, no site-specific vegetation indices were required to run the regional-scale version of PnET-IIS. The same species-specific vegetation coefficients used at the smaller spatial scales were used for regional-scale modeling (Table 2).

Soils Data

Soil water holding capacity, the only soil parameter needed to run PnET-IIS, was derived from a GIS-based Soils Atlas compiled by the Soil Conservation Service (Marx, 1988). In developing a coverage of average SWHC on a 0.5° x 0.5° grid cell, soils unsuitable for growing southern pines were excluded from the data set. If all SWHC soil series values were averaged across a grid cell, very low and high SWHC areas would have been averaged within the same grid cell. This would have produced a cell with an average SWHC that appeared suitable for pine growth. To eliminate this source of input error, we used Forest Inventory and Analysis (FLA) data, which contained stand volume, growth, and species composition information remeasured at more than 21,000 permanent plots across the southern U.S. A database subset that contained plot locations of loblolly pine FLA plots across the southern U.S. was selected. A GIS placed a soil series map for the region over the FLA plot locations. This information provided the associated range of SWHC where the pines were growing. Loblolly pine sites were on FIA plots with a SWHC ranging from 3.8 to 15.8 cm H_2O for soil depths of 102 cm.

Using the selected range of SWHC where loblolly pine grow, a grid of 0.5° x 0.5° cells was placed over the regional map and a weighted average of all remaining SWHC polygons within each cell was computed.

Hydrologic Validation

Researchers have long used U.S. Geologic Survey (USGS) stream flow data for hydrologic modeling, but the emphasis was on model calibration (James, 1972; Dawdy et al., 1972; Magette et al., 1976). Basin streamflow data are useful in broad-scale modeling, calibration, and validation because measurements integrate ecosystem water input, movement, and usage. The USGS has more than 6,000 stream gauging stations across the continental U.S. (USGS, 1992). Average annual run-off data for the southern U.S. was calculated from gauge station data from 1951 to 1980 (Moody et al., 1986). The 0.5° x 0.5° cells were placed over an isopleth map of measured run-off, and a weighted average of mean cell run-off was calculated based on the area size and value of all isopleths within each cell.

Forest Growth Measurements

Model validation at the regional scale was difficult because data are rarely collected over large geographic regions. The FIA database was one source of productivity data that covered a long temporal period for the whole region. The FIA program was established to develop, analyze, and maintain forest resource information needed to formulate policies and programs. The program established more than 21,000 permanent plots across the southern U.S., which are measured every 8 to 10 years. The methods used for measuring each plot have remained unchanged since the 1970s (Kelly, 1991).

Forest inventory and analysis plot selection followed the same site criteria as the previously described ecosystem-level modeling. Forest type, volume, and disturbance (e.g., insect, disease, fire) were recorded for all trees greater than 2.5 cm d.b.h. within each plot. Because the position of each tree was recorded, tree mortality and regeneration were calculated. The FIA plots across Georgia were the only resampled plots that met our selection criteria.

Approximately 170 FIA plots that contained loblolly pine were selected throughout Georgia between 1972 and 1982. However, before the FIA database could be used for model validation, additional data screening was required. PnET-IIS assumed that the plots had a closed canopy. FIA pine plots were classified as seedling, sapling, pole timber, and saw log (>20 cm d.b.h.). For model productivity validation, only sites that were most likely to have a closed canopy at the beginning of the measurement period (i.e., saw log size timber) were compared with PnET-IIS predictions of growth. Additionally, to better represent average growth within each 0.5° x 0.5° grid cell, at least two FIA plots were required per cell. These two selection criteria reduced the original FIA data set to 47 plots. From 1972 to 1982, 19 cells across Georgia contained FIA plots meeting the selection criteria. Measured basal area growth was calculated for each FIA plot by subtracting the 1972 basal area from the 1982 basal area. The resulting value was divided by 10 to estimate annual basal area growth per plot. Average annual basal area growth was summed across all FIA plots within each cell and divided by the number of plots per cell to estimate average annual basal area growth by cell. These values ranged from 5.5 to 18 $cm^2\ tree^{-1}\ cell^{-1}$. To examine the FIA plot growth data at the same temporal scale as model outputs, PnET-IIS predicted NPP was averaged between 1972 and 1982 for each grid cell.

PnET-HS Predicted vs. Measured Hydrology

PnET-IIS predicted that the lowest drainage occurred in eastern Texas and along the Coastal Plain while the highest drainage occurred in the high elevation Appalachian Mountains in southwestern North Carolina and northeastern Georgia (Plate 5*). Although run-off was most strongly determined by precipitation, many factors affect run-off across the region. Nationally, 8% of all run-off was removed for industrial, commercial, and residential purposes (USGS, 1992). Regional location and proximity to population centers also affected the percentage of run-off diverted

* Color plates follow numbered page 168.

from discharge. The other principal factor affecting run-off was vegetation. On average, 50% of precipitation either evaporated from leaf surfaces or transpired through plant stomates. Species type, age, and morphology also influenced ET. Even though some of these factors were not accounted for by PnET-IIS, historic (1951 to 1980) rates of predicted annual run-off generally agreed with the USGS run-off across the region ($r^2 = 0.64$, $P < 0.0001$, $n = 502$) (Figure 6).

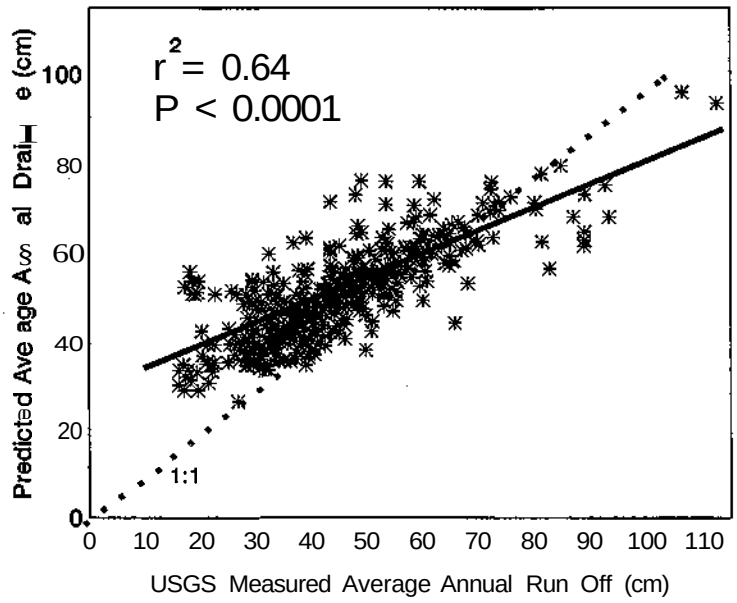

Figure 6 USGS measured average annual historic (1951 to 1980) run-off vs. PnET-IIS predicted average annual water drainage from 1951 to 1980 for the southern U.S.

Comparison of PnET-IIS Predicted vs. Measured Forest Growth

Regional average annual NPP ranged from 4.0 to 16.0 t ha^{-1} yr^{-1} between 1951 and 1984. The largest predicted productivity occurred across the southern and eastern coastal areas, and the smallest predicted productive areas were in the northern and western loblolly pine range (Plate 6*).

Teskey et al. (1987) measured a range of above-ground NPP between 2 and 10 t ha^{-1} yr^{-1} on loblolly pine sites. Other studies have estimated that below-ground production equals approximately 40% of above-ground NPP (Nadelhoffer et al., 1985; Whittaker and Marks, 1975). Multiplying Teskey et al. (1987) measurements of above-ground NPP by 1.4 (60% above-ground NPP/40% below-ground NPP) yielded a measured range of total (above-ground and below-ground) NPP between 3.0 and 15.0 t ha^{-1} yr^{-1}, with most site NPP (above-ground only) >8.5 t ha^{-1} yr^{-1} (Teskey et al., 1987). PnET-IIS predicted NPP ranged from 2 to 18 t ha^{-1} yr^{-1}, with the average annual >9 t ha^{-1} yr^{-1}. Although NPP was always positive annually, the

* Color plates follow numbered page 168.

model predicted that NPP would be negative on some sites during the hottest months when average monthly maximum air temperature >30°C.

Across Georgia, predicted average annual NPP ranged from 9.5 to 15.5 t ha^{-1} with most of the values between 9.7 and 14.5 t ha^{-1} yr^{-1}. Forest inventory and analysis annual basal area growth per plot for the state ranged from 9.8 to 15.4 cm, which was significantly correlated with predicted NPP (r^2 = 0.70, P < 0.0001, Figure 7).

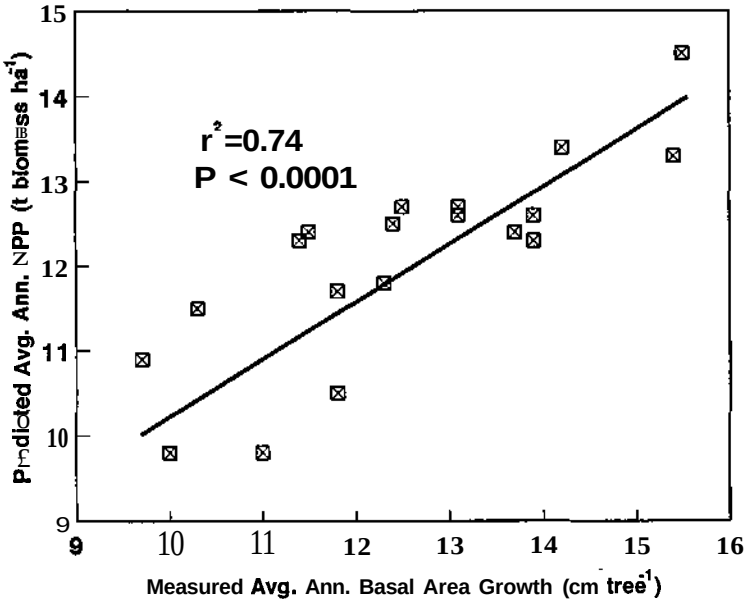

Figure 7 Correlation between predicted average annual NPP and FIA measured average annual basal area growth across Georgia from 1972 to 1982.

Summary Regional Modeling

Many model assumptions and parameter aggregations were required to operate PnET-IIS at a regional scale. Despite these conditions, PnET-IIS predictions of regional scale forest hydrology and productivity were well correlated with available validation data. The spatial scale of the regional model (i.e., 50 x 75 km) was small enough to minimize the model prediction error associated with spatial aggregation of the climate data.

PnET-IIS predictions of forest growth and hydrology were compared using aggregated validation data. Therefore, both the validation data and model prediction may have been biased due to the aggregation. The potential for bias in the validation data does not preclude its use for comparison with model predictions, but the reader should understand that the validation data may not accurately represent environmental conditions at the finer scale.

CONCLUSIONS

The amount of predictive error associated with data aggregation is dependent on the scale for which the model was developed and applied. In this example, the predictive capability of the ecosystem-level model PnET-IIS was compared with measured forest growth and hydrology from three spatial scales. PnET-IIS predictions of drainage and ET were poorly correlated with stand-level measured data and predictions of hydrology using the stand-level hydrologic model PROSPER. The lack of a deep soil water storage term and daily to monthly aggregation of the climate data reduced the accuracy of stand-level predictions of hydrology. PnET-IIS was a better predictor of forest growth at the ecosystem-level. Regional predictions of drainage were well correlated with measured regional-scale stream flow, and FIA measured loblolly pine growth was correlated with predicted NPP. The model was insensitive to SWHC and climate spatial aggregation. Predictions of NPP and forest hydrology were not always well correlated with measured processes for each site, but the model predicted generally well across all sites. The aggregation of both the input data and the validation data may have biased the model predictive accuracy and our ability to assess the models' performance. Temporal and spatial aggregation can substantially influence model predictions and should be considered when applying or validating a model across multiple scales.

ACKNOWLEDGMENTS

The authors thank Eugene Pape for technical support, John Aber for assistance in model use and modification, three anonymous reviewers, and Teresa Moss for assistance in manuscript preparation. Support for this research was provided by the USDA Forest Service Southern Global Climate Change Program.

REFERENCES

Aber, J. D. and Federer, C. A., A generalized, lumped-parameter model of photosynthesis, evapotranspiration and net primary production in temperate and boreal forest ecosystems, *Oecologia*, 92, 463, 1992.

Aber, J. D., Ollinger S. V., Federer C. A., Reich P. B., Goulden M. L., Kicklighter D. W., Melillo J. M., and Lathrop R. G., Jr., Predicting the effects of climate change on water yield and forest production in the northeastern U.S., *Climate Res.*, 5, 207, 1995.

Band, L. E., Effect of land surface representation on forest water and carbon budgets, *J. Hydrol.*, 150, 749, 1993.

Caldwell, M. M., Matson, P. A., Wessman, C., and Gammon, J., Prospects for scaling, in *Scaling Physiological Processes*, Ehleringer, J. R. and Field, C., Eds., Academic Press, San Diego, 223, 1993.

Dawdy, D. R., Lichty, R. W., and Bergmann, J. M., A rainfall-runoff simulation model for estimation of flood peaks for small drainage basins, USGS Professional Paper 506-B, 1972.

Faulkner, P., Schoeneberger, M. M., and Kress, L. W., Below ground changes in loblolly pine as indicators of ozone stress, in *Proc. 6th Biennial Southern Silvicultural Res. Conf.*, Memphis, TO, 332, 1990.

Goldstein, R. A., Mankin, J. B., and Luxmoore, R. J., Documentation of PROSPER: A model of atmosphere-plant-soil water flow, Oak Ridge National Laboratory, Oak Ridge, TN, 1974.

Huff, D. W. and Swank, W. T., Modeling changes in forest evapotranspiration, in *Hydrological Forecasting*, Anderson, M. G. and Burt, T. P., Eds., John Wiley & Sons, New York, 1985, 121.

James, L. D., Hydrologic modeling, parameter estimation, and watershed characteristics, *J. Hydrol.*, 17, 283, 1972.

Kelly, J. R, USDA forest survey methods, in *Proc. Alabama's Forest Resour.: Past, Present and Future*, Jones, R. H., Ed., Auburn University, 7, 1991.

Kramer, P. J., Drought, stress and the origin of adaptations, in *Adaptation of Plants to Water and High Temperature Stress*, Turner, N. C., and Kramer, P. J., Eds., John Wiley & Sons, New York, 1980.

Kress, L. W., Allen, H. L., Mudano, J. E., and Stow, T. K., Impact of ozone on loblolly pine seedling foliage production and retention, *Environ. Toxicol. Chem.*, 11, 1115, 1992.

Luxmoore, R. J., Application of the Green and Corey method for computing hydraulic conductivity in hydrologic modeling, Oak Ridge National Laboratory, Oak Ridge, TN, EDFB/IBP-74/4, 1973.

Magette, W. L., Shanholtz, V. O., and Carr, J. C., Estimating selected parameters for the Kentucky Watershed Model from watershed characteristics, *Water Resour. Res.*, 12, 472, 1976.

Marx, D. H., Southern forest atlas project, in *81st Annual Meet. Assoc. Dedicated Air Pollut. Control Hazardous Waste Management*, (APCA), Dallas, Texas, 1988.

McNulty, S. G., Vose, J. M., and Swank, W. T., Modeling loblolly pine hydrology and productivity across the southern United States, *For. Ecol. Manage.*, 1996a, in press.

McNulty, S. G., Vose, J. M., and Swank, W. T, Predictions of net primary production, soil water deficit, evapotranspiration and drainage in southern U.S. loblolly pine stands, *Ambio*, 1996b, in press.

McNulty, S. G., Vose, J. M., and Swank, W. T, Predictions and projections of pine productivity and hydrology in response to climate change across the southern United States, in *Global Change and the Forests of the Southeastern United States*, Springer-Verlag, New York, 1996c, in press.

McNulty, S. G., Vose, J. M., Swank, W. T, Aber, J. D., and Federer, C. A., Regional-scale forest ecosystem modeling: data base development, model predictions and validation using a geographic information system, *Climate Res.*, 4, 223, 1994.

Melillo, J. M., McGuire, A. D., Kicklighter, D. W, Moore III, B., Vorosmarty, C. J., and Schloss, A. L., Global climate change and terrestrial net primary production, *Nature*, 363, 234, 1993.

Mintzer, I. M., Energy, greenhouse gases, and climate change, *Ann. Rev. Energy*, 15, 513, 1990.

Mitchell, M. J., David, M. B., and Harrison, R. B., Sulfur dynamics of forest ecosystems, in *Sulfur Cycling in Terrestrial Ecosystems and Wetlands*, John Wiley & Sons, New York, 1989, 42.

Moody, D. W, Chase, E. B., and Aronson, D. A., National Water Summary 1985 Hydrologic Events and Surface-Water Resources, USGS Water-Supply Paper 2300, US Government Printing Office, Washington, D.C., 1986.

Nadelhoffer, K., Aber, J. D., and Melillo, J. M., Fine roots, net primary production, and soil nitrogen availability: a new hypothesis, *Ecology*, 66, 1377, 1985.

Nikolov, N. T. and Zeller, K. E, A solar radiation algorithm for ecosystem dynamic models, *Ecol. Model*, 61, 149, 1992.

Running, S. W. and Gower, S. T., Forest-BGC, A general model of forest ecosystem processes for regional applications. II. Dynamic carbon allocation and nitrogen budgets, *Tree Physiol.*, *9*, 147, 1991.

Strain, B. R., Higginbotham, K. O., and Mulroy, J. C., Temperature preconditioning and photosynthetic capacity of *Pinus taeda L.*, *Photosynthetica*, 10, 47, 1976.

Swank, W. T., Swift, Jr., L. W., and Douglass, J. E., Streamflow changes associated with forest cutting species conversions and natural disturbances, in *Forest Hydrology and Ecology at Coweeta*, Swank, W. T., and Crossley Jr., D. A., Eds., Springer-Verlag, New York, 1988, 297.

Swift, Jr., L. W., Swank, W. T., Mankin, J. B., Luxmoore, R. J., and Goldstein, R. A., Simulation of evapotranspiration and drainage from mature and clear-cut forest and young pine plantations, *Water Resour. Res.*, 11(5), 667, 1975.

Swift, Jr., L. W., Algorithm for solar radiation on mountain slopes, *Water Resour. Res.*, 12, 108, 1976.

Swift, Jr., L. W., Cunningham, G. B., and Douglas, J. E., Climatology and hydrology, in *Forest Hydrology and Ecology at Coweeta*, Swank, W. T., and Crossley, Jr., D. A., Eds., Springer-Verlag, New York, 1988, 35.

Swift, Jr., L. W., Waide, J. B., and White, D. L., Refinements in the Z-T method of extreme event analysis for small watersheds, in *6th Conf. Appl. Climatol.*, American Meteorological Society, Charleston, SC, 60, 1989.

Teskey, R. O., Bongarten, B. C., Cregg, B. M., Dougherty, P. M., and Hennessey, T. C., Physiology and genetics of tree growth response to moisture and temperature stress: an examination of the characteristics of loblolly pine *(Pinus taeda* L.), *Tree Physiol.*, 3, 41, 1987.

US Geological Survey, Regional hydrology and the USGS stream gaging network, National Academy Press, Washington, D.C., 1992.

Vose, J. M., and Swank, W. T., Effects of long-term drought on the hydrology and growth of a white pine plantation in the southern Appalachians, *For. Ecol. Manage.*, 64, 25, 1994.

Wessman, C. A., Spatial scales and global change: Bridging the gap from plots to GCM grid cells, *Ann. Rev. Ecol. Sys.*, 23, 175, 1992.

Whittaker, R. H., and Marks, P. L., Methods of assessing terrestrial productivity, in *Primary Production of the Biosphere*, Lieth, H. and Whittaker, R. H., Eds., Springer-Verlag, New York, 1975.

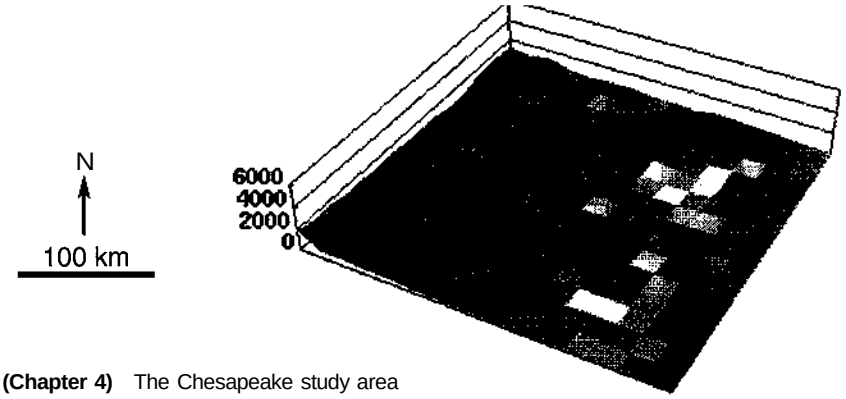

Plate 1 (Chapter 4) The Chesapeake study area shown as perspective renderings at level 9 (16,000 m) and level 5 (1,000 m) with AVHRR NDVI values draped on digital elevation data, elevations in meters.

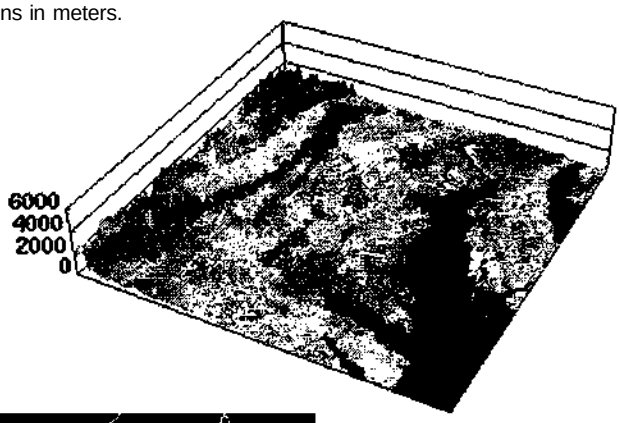

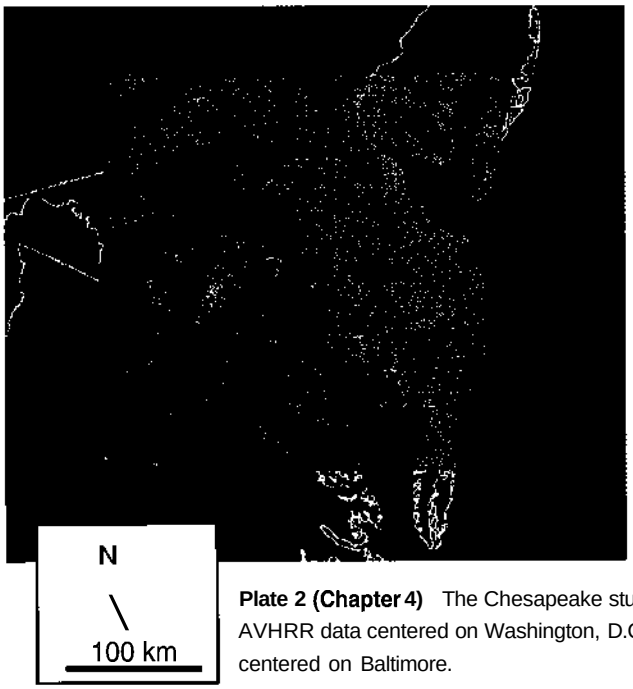

Plate 2 (Chapter 4) The Chesapeake study area showing 1-km AVHRR data centered on Washington, D.C. and 28.5-m TM data centered on Baltimore.

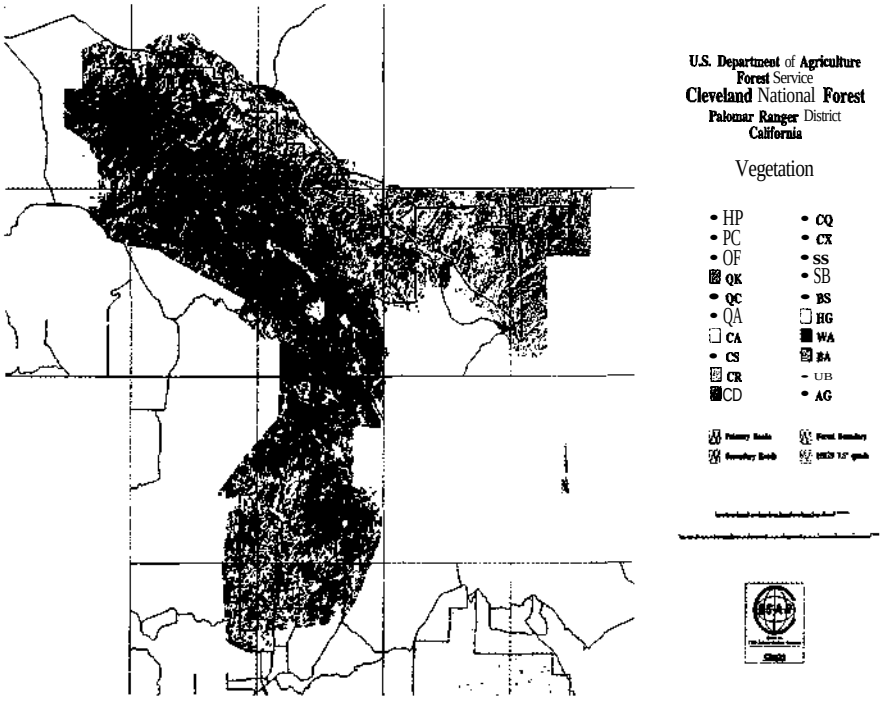

Plate 3 (Chapter 7) Forest Service stand-based vegetation map for the Palomar study area (se Table 1 for a key to the vegetation classes listed in the legend).

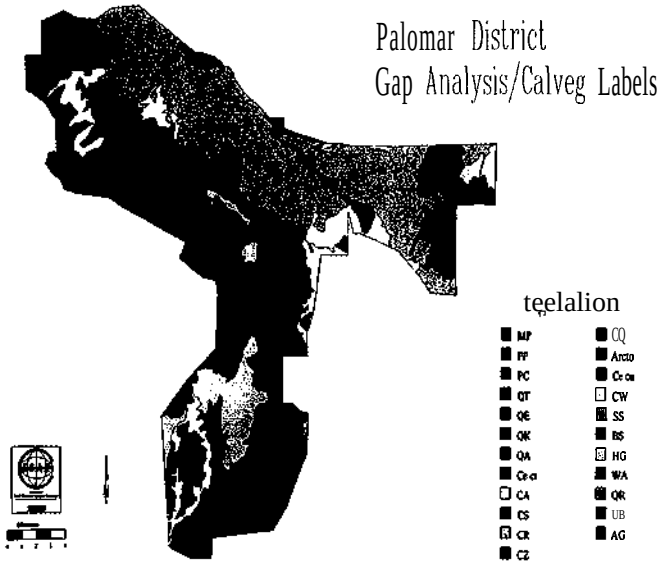

Plate 4 (Chapter 7) A portion of the California Gap Analysis program vegetation map for the southwest Ecoregion (Davis et al., 1994) corresponding to the Palomar study area (see Tables 1 and 4 for a key to the vegetation classes listed in the legend).

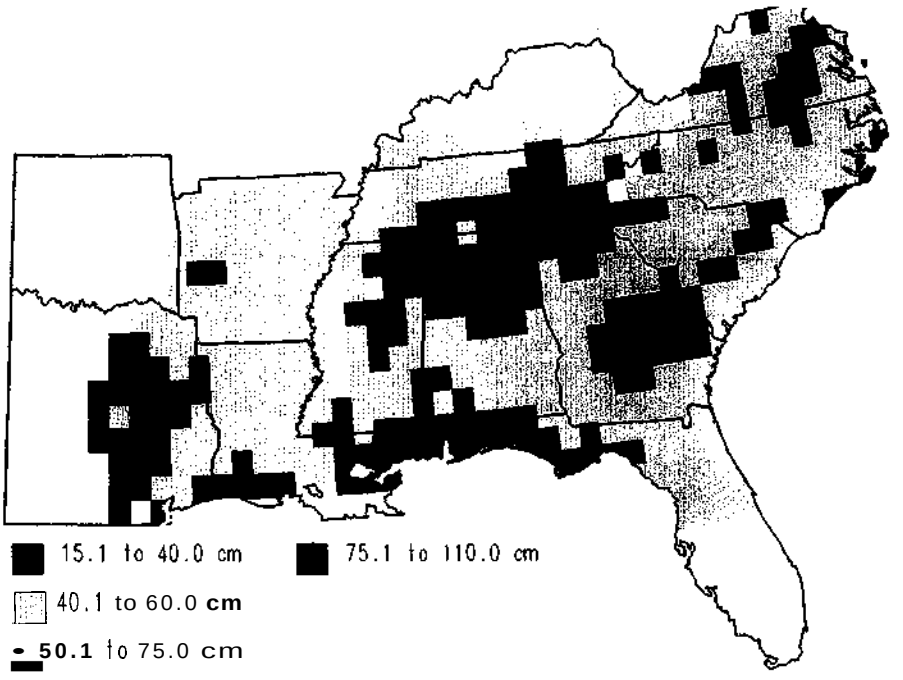

Plate 5 (Chapter 9) PnET-IIS predicted average annual water drainage using historic (1951 to 1980) climate data.

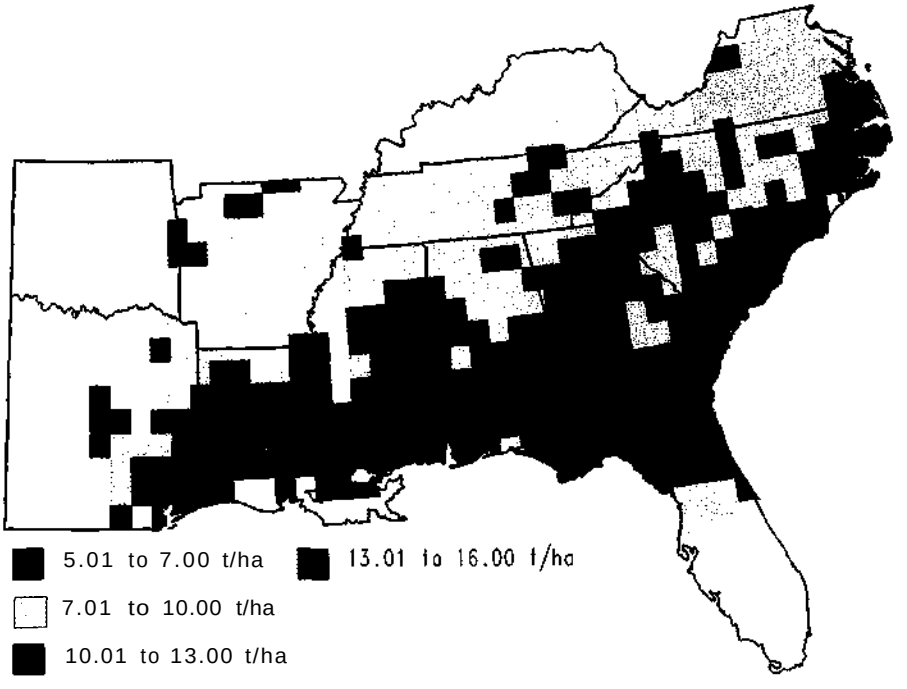

Plate 6 (Chapter 9) PnET-IIS predicted average annual net primary productivity using historic (1951 to 1980) climate data.

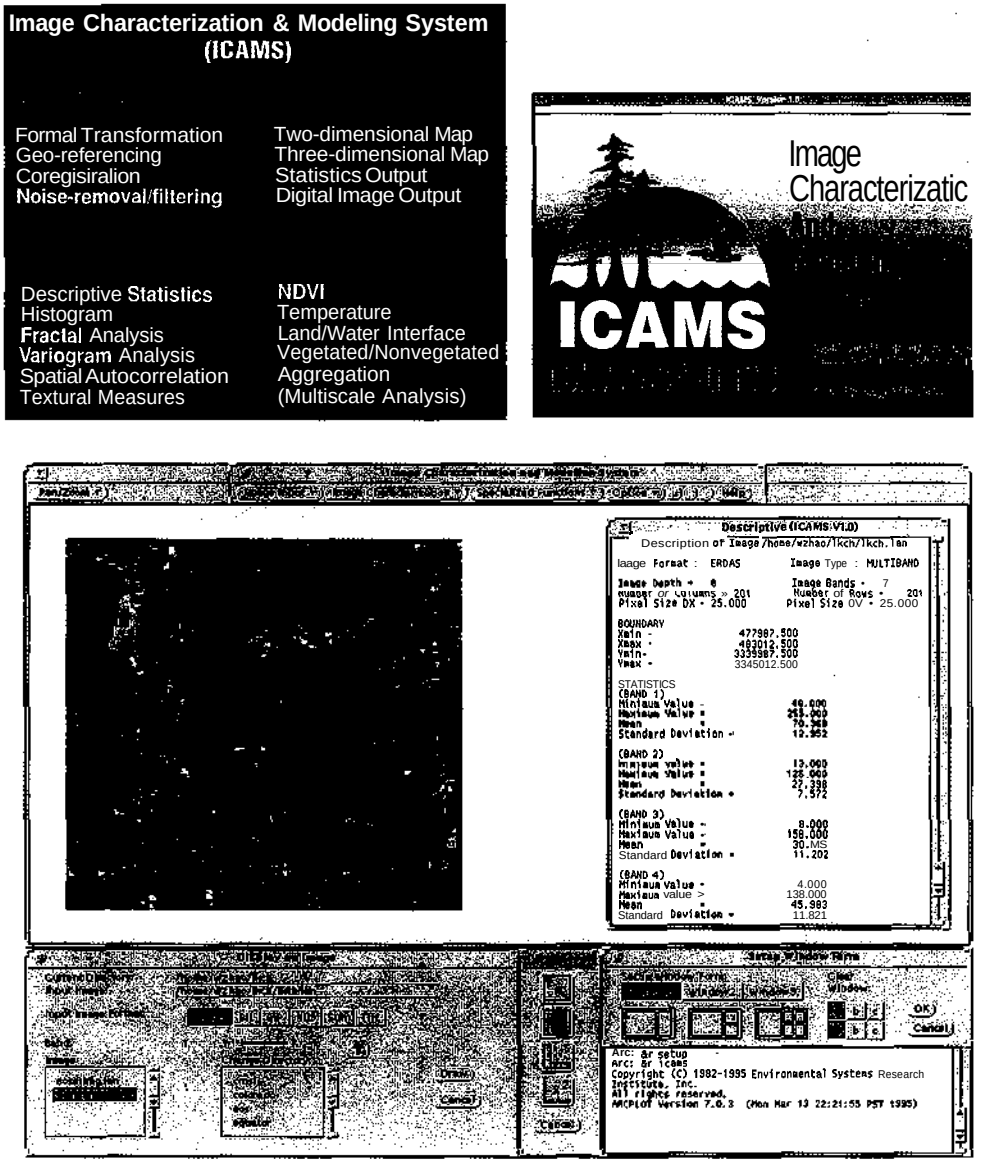

Plate 7 (Chapter 14)

Upper left. Image display of ICAMS subsystem processing functions.

Upper right. ICAMS opening logo.

Bottom. Display of Lake Charles, Louisiana TM image and basic descriptive statistics.

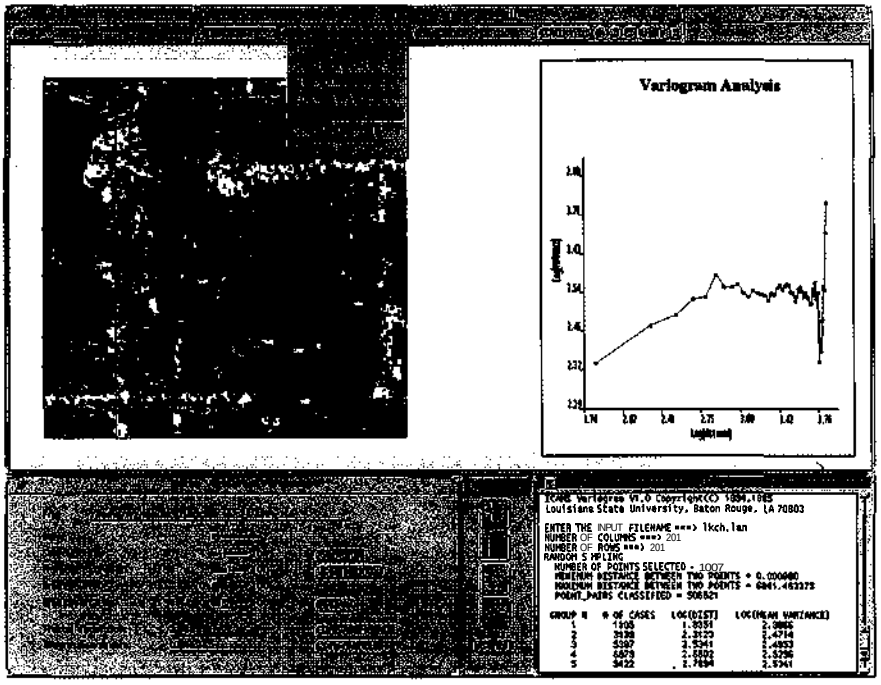

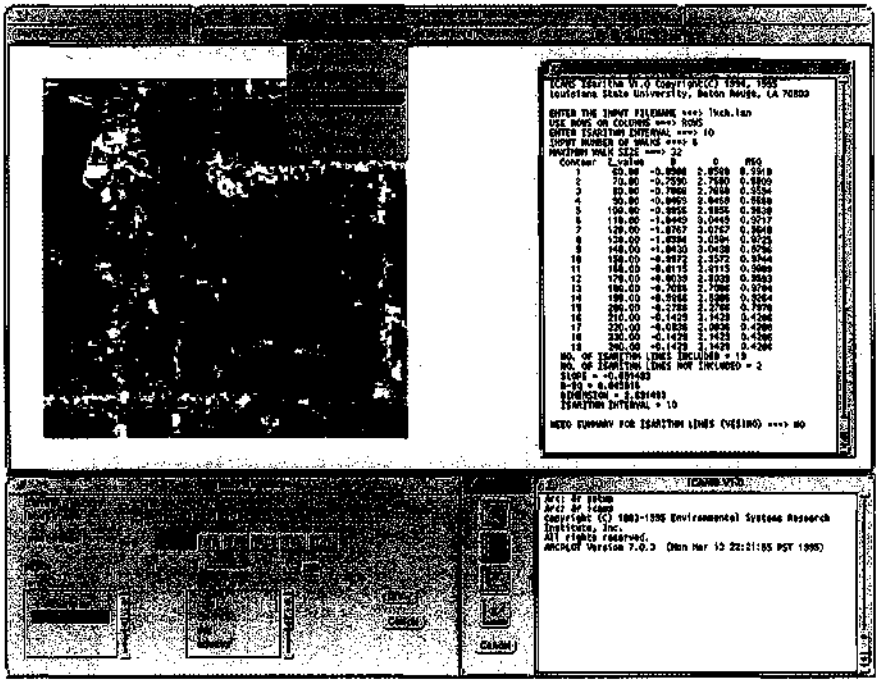

Plate 8 (Chapter 14)

Top. ICAMS variogram fractal analysis of Lake Charles, Louisiana TM image.

Bottom. ICAMS isarithm fractal analysis of Lake Charles, Louisiana TM image.

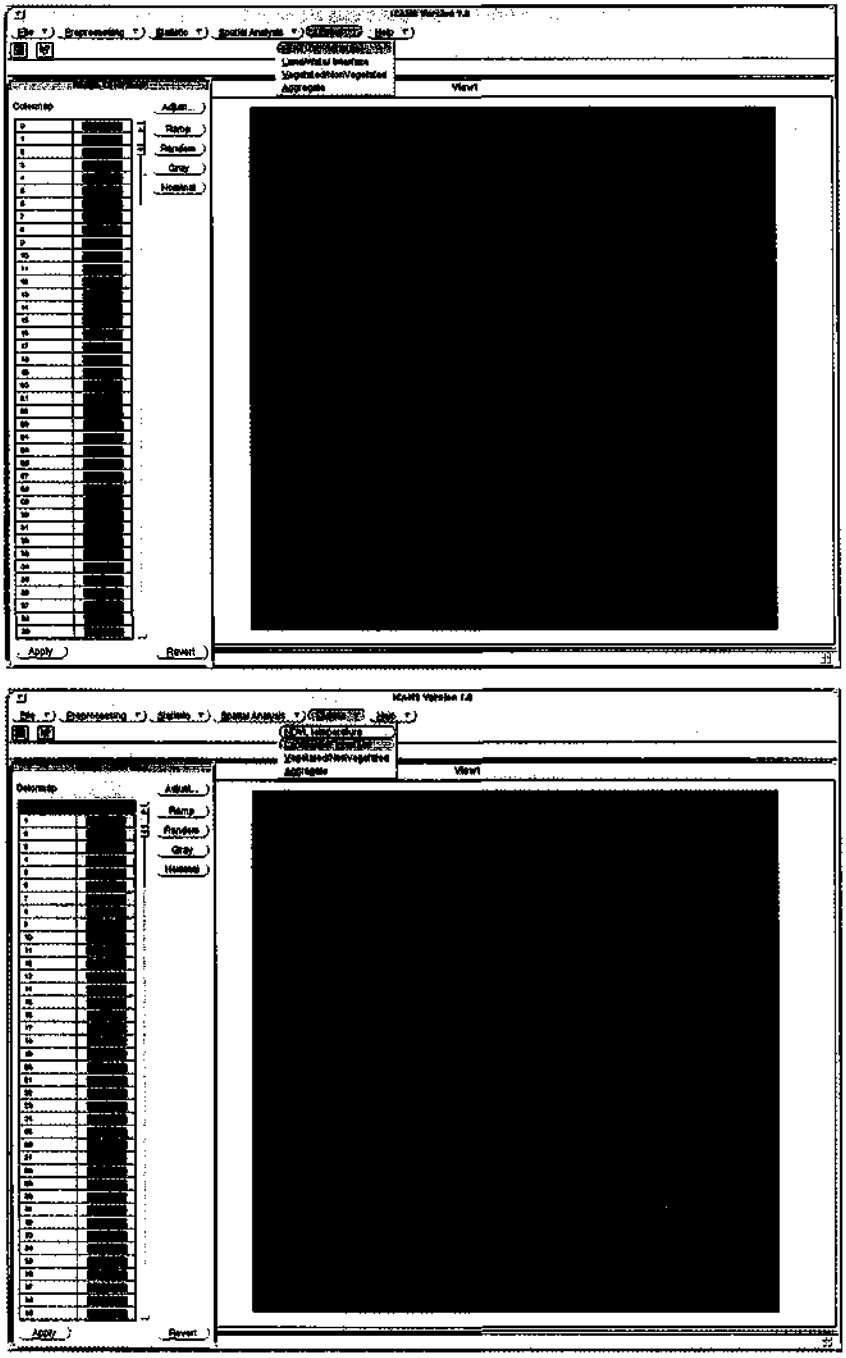

Plate 9 (Chapter 14)

Top. ICAMS NDVI computation of Lake Charles, Louisiana TM image. Green indicates higher NDVI values; blue indicates lower NDVI values.

Bottom. ICAMS land versus water delineation of Lake Charles, Louisiana TM image. Blue is water; green is land.

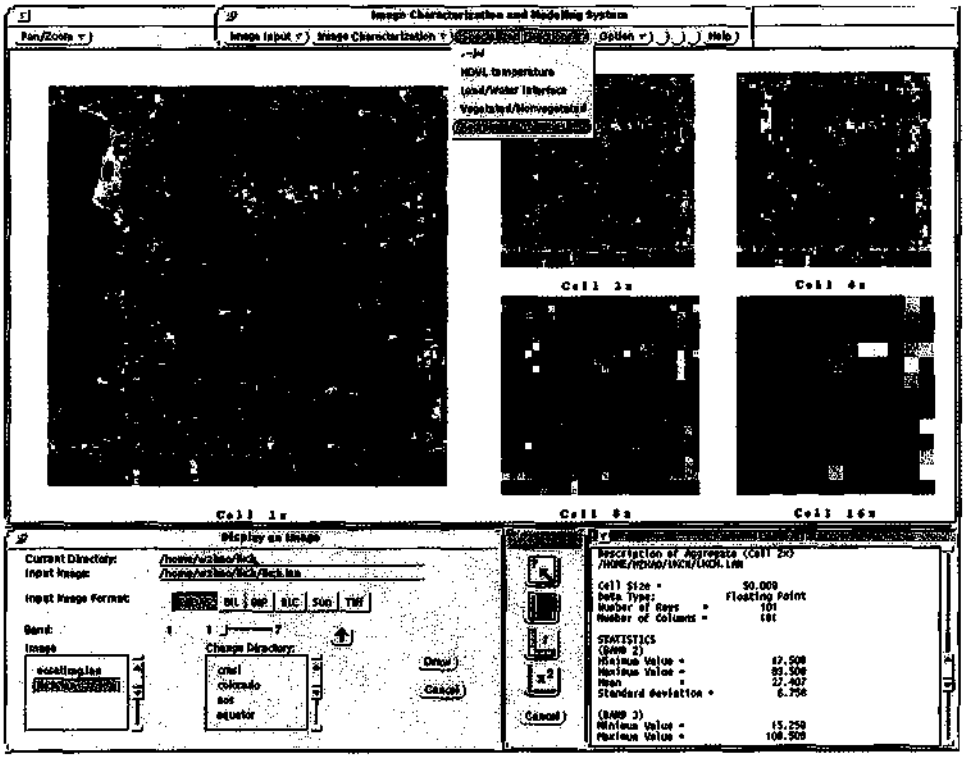

Plate **10** (Chapter 14) ICAMS aggregation of Lake Charles, Louisiana TM image from 2x2 to 16x1 aggregation.

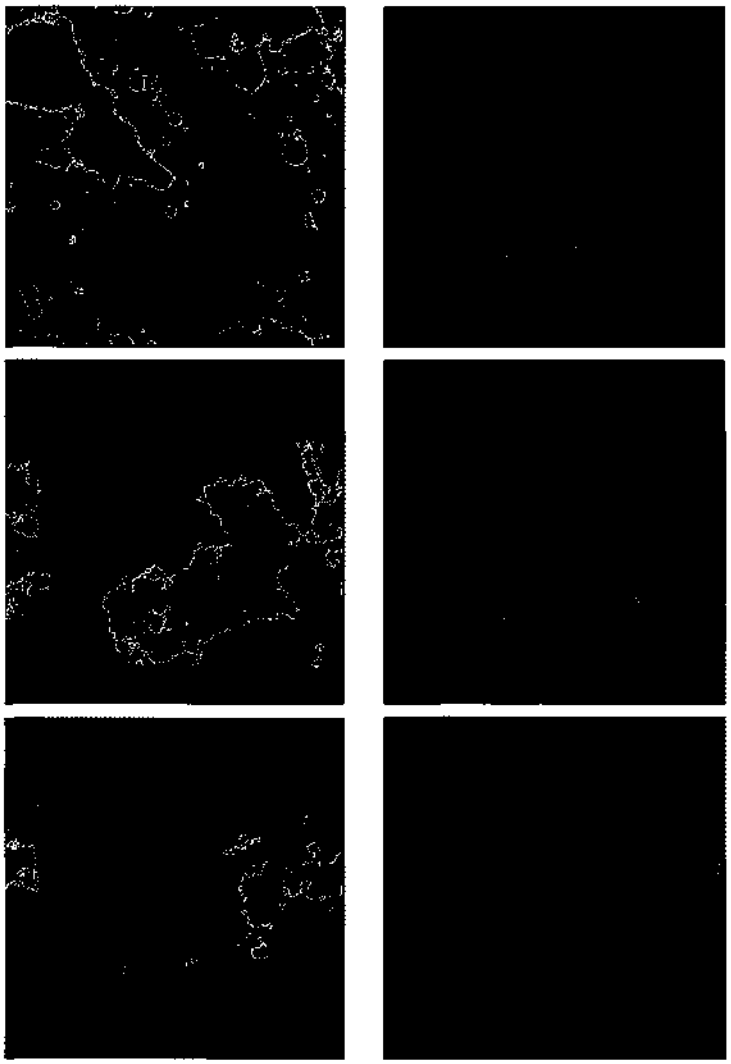

Plate 11 (Chapter 16) Simulated fields with varying multifractal parameters. The palette is rainbow, with high values red and low values purple. From top to bottom, a = 0.06, 1.2, and 1.8. C_1 = 0.05 on the left and 1.2 on the right.

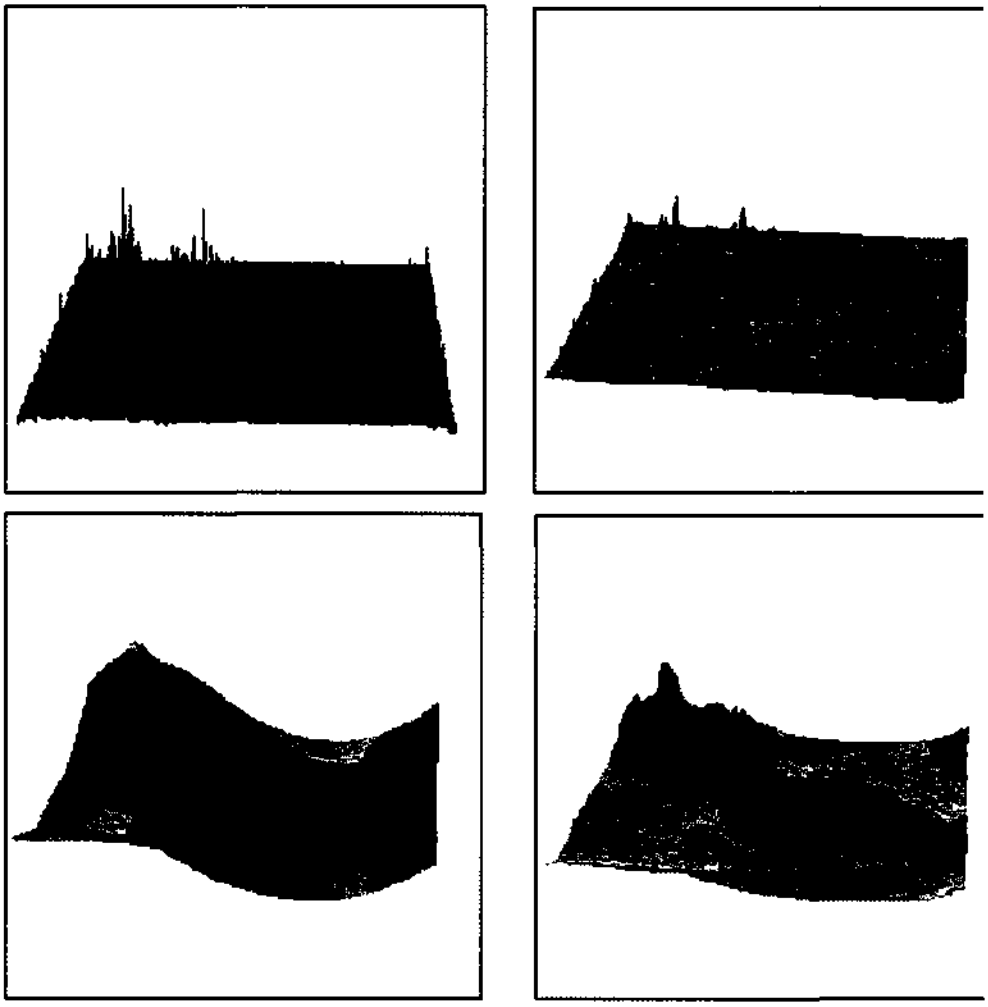

Plate 12 (Chapter 16) Varying the H-filter of the simulated field: a = 1.7, $H = 0.05$. Clockwise from tc left $H = -1.0$, $H = 0.0$, $H = 1.0$, $H = 2.0$

STEP 1: Generate a Levy noise at each point, with the parameters a, a measure of the multifractality of the field, and C_1, the sparseness of the mean of the field.

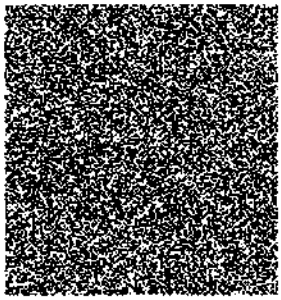

STEP 2: Fourier transform the noise.

STEP 3: Generate a filter I k I$^{-d/\alpha'}$, with anisotropies given by the GSI parameters (using an anistropic norm); multiply the noise by this.

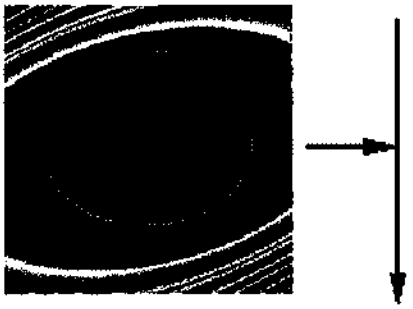

STEP 4: Inverse fourier transform the result. Steps 2 through 4 are the equivalent of a convolution of the noise with the appropriate filter.

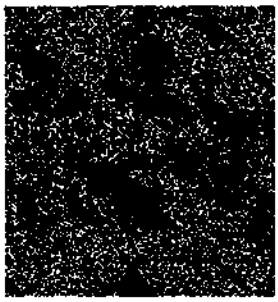

STEP 5: Exponentiate to obtain a real field.

STEP 6: Spectrally filter the field with a I k I^{-H} filter. This scale-invariant smoothing is in fact a fractional integration.

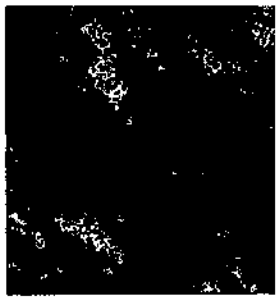

Plate 13 (Chapter 16) Simulating a universal multifractal field.

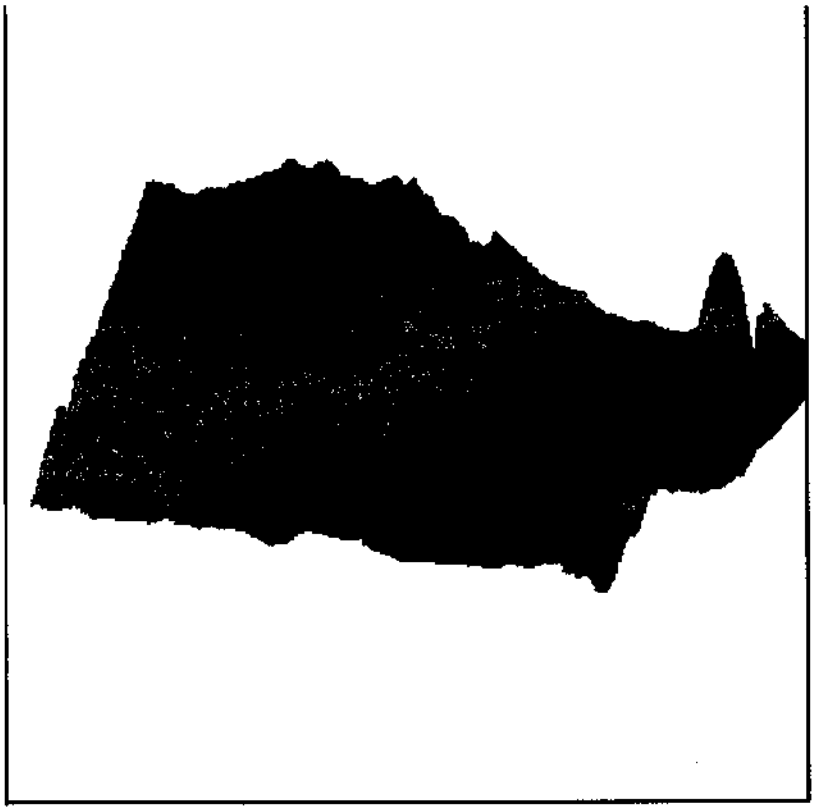

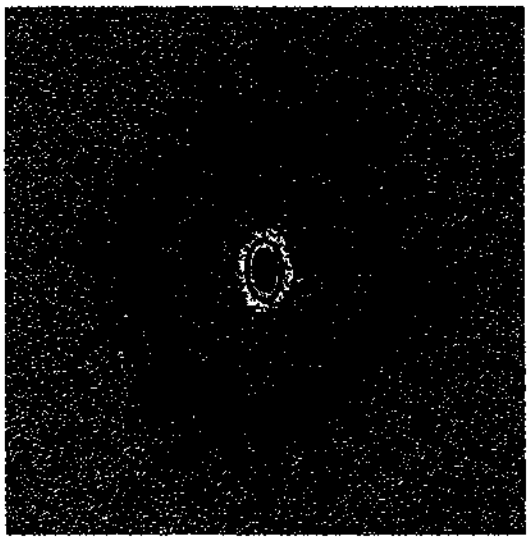

Plate 14 (Chapter 16)

Top. An example of U.S. landscape topography data, with 90-m resolution and size 512 x 512, visualized with ray-tracing. High values are brown; low values are green.

Bottom. The 2-D power spectrum of the data, showing anisotropies by the non-circular shapes. GSI parameters are c = 0.15, $f = -0.10$, and $e = 0.04$. The theoretical balls have been overlaid.

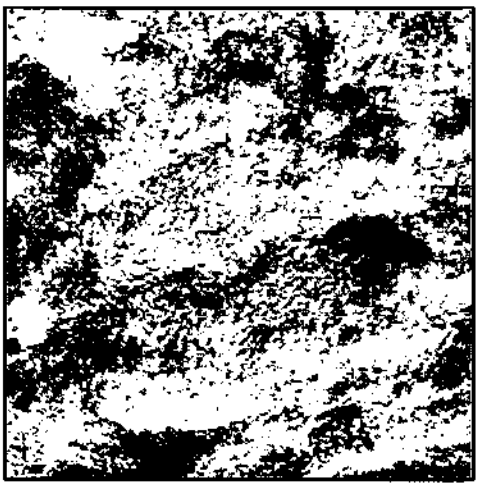

Plate 17 (Chapter 16)
Comparison of cumulus cloud data (top) with simulated cumulus (right top and bottom), using the measured parameters:
a = 1.13, C_1 = 0.09, H = 0.4 and GSI parameters of c= 0.10, f = -0.5, and e = 0.30, with a spheroscale of ~ 30km.

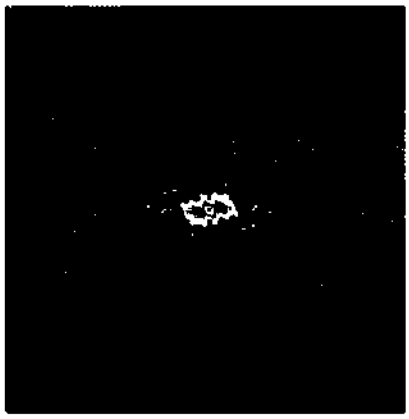

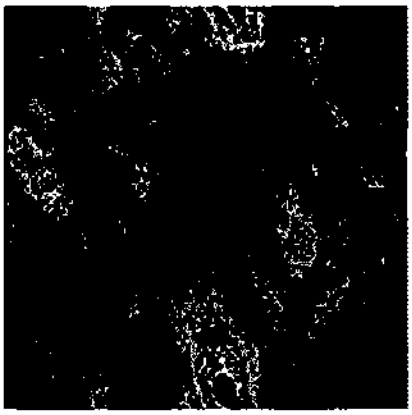

Plate 18 (Chapter 16)
Aeromagnetic anomaly data. Clockwise from top left, an aeromagnetic anomaly data set, its 2-D power spectrum, and a simulated field made using the measured parameters: $\alpha = 1.9$, $C_1 = 0.15$, and $H = 0.65$; and $c = 0.05$, $f = 0.10$, and $e = 0.22$. Note that for larger scales, the noise in the power spectrum of the data set alters the apparent shape of the balls.

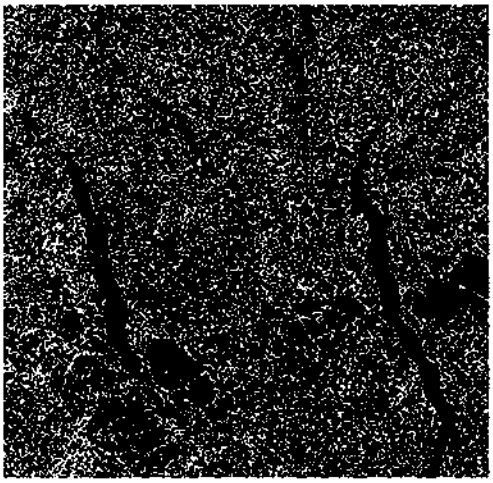

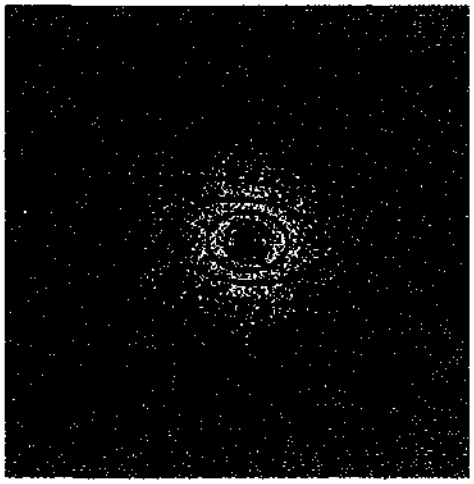

Plate 19 (Chapter 16) Sea ice radar reflectivity data. On the left is a data set, C band, polarization H with resolution of 12.5 m and size 512 x 512. On the right is its 2-D power spectrum. The GSI parameters measured were $c = 0.21$, $f = 0.0$, and $e = 0.0$.

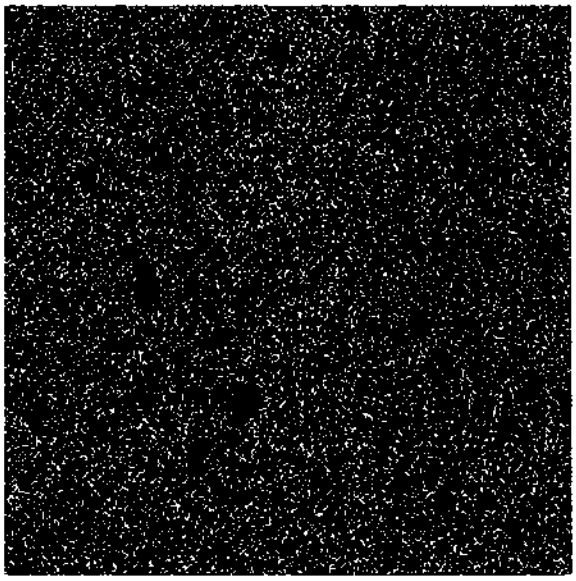

Plate 20 (Chapter 16) An example of simulated sea ice radar reflectivity, using a = 1.85, C_1 = 0.01, H= -0.10. The GSI parameters used were c= 0.21, f= 0.0, and e = 0.0.

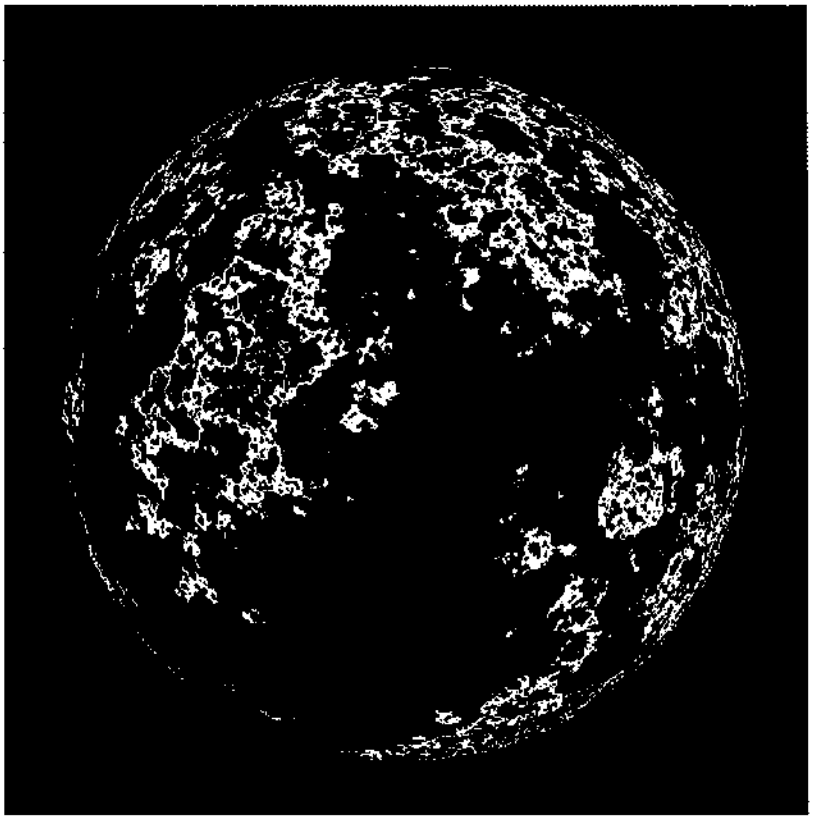

Plate 21 (Chapter 16) An example of simulated topography on a spherical surface (from Tan et al., 1996). Here, α = 1.7, C_1 = 0.10, H = 0.5.